Computer Modeling in Engineering & Sciences

Tech Science Press

DOI: 10.32604/cmes.2024.059552

ARTICLE

SEIR Mathematical Model for Influenza-Corona Co-Infection with Treatment and Hospitalization Compartments and Optimal Control Strategies

Muhammad Imran[1,*], Brett McKinney[1] and Azhar Iqbal Kashif Butt[2]

[1]Tandy School of Computer Science, University of Tulsa, Tulsa, OK 74104, USA

[2]Department of Mathematics and Statistics, College of Science, King Faisal University, Al-Ahsa, 31982, Saudi Arabia

*Corresponding Author: Muhammad Imran. Email: muhammad-imran@utulsa.edu

Received: 11 October 2024 Accepted: 09 December 2024 Published: 27 January 2025

ABSTRACT

The co-infection of corona and influenza viruses has emerged as a significant threat to global public health due to their shared modes of transmission and overlapping clinical symptoms. This article presents a novel mathematical model that addresses the dynamics of this co-infection by extending the SEIR (Susceptible-Exposed-Infectious-Recovered) framework to incorporate treatment and hospitalization compartments. The population is divided into eight compartments, with infectious individuals further categorized into influenza infectious, corona infectious, and co-infection cases. The proposed mathematical model is constrained to adhere to fundamental epidemiological properties, such as non-negativity and boundedness within a feasible region. Additionally, the model is demonstrated to be well-posed with a unique solution. Equilibrium points, including the disease-free and endemic equilibria, are identified, and various properties related to these equilibrium points, such as the basic reproduction number, are determined. Local and global sensitivity analyses are performed to identify the parameters that highly influence disease dynamics and the reproduction number. Knowing the most influential parameters is crucial for understanding their impact on the co-infection's spread and severity. Furthermore, an optimal control problem is defined to minimize disease transmission and to control strategy costs. The purpose of our study is to identify the most effective (optimal) control strategies for mitigating the spread of the co-infection with minimum cost of the controls. The results illustrate the effectiveness of the implemented control strategies in managing the co-infection's impact on the population's health. This mathematical modeling and control strategy framework provides valuable tools for understanding and combating the dual threat of corona and influenza co-infection, helping public health authorities and policymakers make informed decisions in the face of these intertwined epidemics.

KEYWORDS

Influenza-corona co-infection; stability analysis; sensitivity analysis; treatment; self-precaution; optimal control

1 Introduction

Coronavirus or COVID-19 first reported in Wuhan, China, in late 2019 [1,2]. The World Health Organization officially declared the COVID-19 pandemic in March 2020 [3,4], following a series of devastating coronaviruses, such as SARS-CoV and MERS-CoV, that had already spread globally

[5,6]. The coronavirus can lead to a deadly cytokine storm, similar to previous coronaviruses [7–9]. The available evidence indicates that the primary mode of transmission of the coronavirus among individuals is through the release of respiratory droplets during activities such as sneezing and coughing [10]. The incubation period for the coronavirus disease typically ranges from 2 to 14 days, with an average of 5 to 6 days [11]. Influenza, commonly called the flu, is an infectious respiratory disease caused by the influenza virus [12,13]. During seasonal pandemics and epidemics, influenza spreads widely throughout the world. Apart from pandemic influenza, there is a global influenza outbreak every year that causes between 3 and 5 million cases of severe disease and between 250,000 and 500,000 fatalities [14]. The time it takes for the signs and symptoms of influenza to appear is about 2 days but might range from 1 to 4 days [15].

Concerns about the possibility of a twin epidemic of influenza and corona have persisted since the start of the pandemic. Many cases have been reported where individuals had both SARS-CoV-2 and influenza [16]. Up to 20% of corona patients, according to some research [17], can have co-infections with other respiratory viruses. The influenza season and the corona pandemic pose a significant threat to public health. Both viruses share similar transmission characteristics and clinical symptoms, causing respiratory infections [17]. The interplay between influenza and corona viruses is a major concern, with fatalities among people infected with both viruses being twice as high as those infected with the new coronavirus [16,17].

Co-infection between corona and other respiratory pathogens is more common in the USA and China, with 7% of SARS-CoV-2-positive patients sharing the burden of co-infection [17]. The clinical signs of corona and influenza include coughing, runny noses, sore throats, fevers, headaches, and fatigue [16,17]. Those who are infected with either virus can experience varied levels of illness, including some who show no symptoms, only minor symptoms, or severe disease [17]. Both the flu and corona can have severe consequences, including pneumonia, respiratory failure, acute respiratory distress syndrome, sepsis, heart attacks or strokes, multiple organ failure, severe inflammation, and even death [18,19].

Both coronavirus and influenza are single-stranded encapsulated RNA viruses; the former contain a positive sense RNA strand and the latter a negative one [20]. Both have comparable infection sites in the upper respiratory tracts (URT) and lower respiratory tracts (LRT). While influenza URT infections are highly transmissible but have a low pathogenicity, influenza LRT infections can produce more severe symptoms [20]. Furthermore, both viruses can spread directly from person to person or indirectly through close contact. Their routes of transmission are comparable and include droplet, aerosol, and self-inoculation by hand contamination [16,17,20]. Co-infection can affect the disease prognosis, increase therapeutic intolerance, and severely compromise the immune system of the host. One of the most important area of epidemiology has been the study of the co-existence and co-infection of multiple diseases [21,22]. To assess the dynamics of co-infection and estimate the treatment facilities, epidemiological models are very helpful. Numerous research works focus on the coexistence of two infectious agents in vulnerable hosts [22–26].

There is a considerable body of work in the literature focusing on coronavirus, influenza, and their co-infection. Epidemiologists are consistently striving to provide comprehensive insights into these epidemics and develop effective control strategies with minimal costs. In [9], the authors formulated an extended susceptible-exposed-symptomatic-asymptomatic-superspreader-quarantine-recovered (*SEIAPQR*) mathematical model, incorporating two non-pharmaceutical optimal control strategies: quarantine and self-precautions. In [21], the authors constructed a model for co-infection of coronavirus and influenza, introducing vaccination compartments for COVID-19, Influenza, and

corona-influenza co-infection. They analyzed the impact of vaccinations, including booster doses for COVID-19, and offered a detailed analysis of influenza-corona co-infection, exploring the effects of transmission, cure, or treatment dynamics. Similarly, in [22], the authors proposed a mathematical model for corona-influenza co-infection, dividing the entire model into three susceptible-exposed-infected-recovered (*SEIR*) submodels with a vaccination compartment. The dynamics of each submodel are analyzed individually to understand the complete model. Finally, an optimal control strategy is defined in [22] with three optimal controls: non-pharmaceutical strategy (minimization of infectious interactions), vaccine for corona, and vaccination for influenza, respectively.

To investigate the co-dynamics of influenza and corona co-infection, we divide the total population into eight distinct time-dependent classes or compartments: susceptible $S(t)$, exposed $E(t)$, infectious with influenza $I_I(t)$, infectious with corona $I_C(t)$, infectious with co-infection $I_{IC}(t)$, under-treatment $T(t)$, hospitalized $H(t)$, and recovered $R(t)$. First we prove fundamental properties (i.e., positive, bounded, and well-posedness) of the proposed model. Then, we determine the important equilibrium points (disease-free equilibrium (DFE) and endemic equilibrium (EE)) of the proposed model, the reproduction number $\mathscr{R}_0$, and demonstrate that DFE and EE points are locally and globally asymptotically stable. To determine the most important critical parameters for $\mathscr{R}_0$, we perform sensitivity analysis and mark the critical parameters for disease control analysis. In the second phase of this study, we will conduct an optimal control analysis aimed at minimizing disease spread [25,26]. To achieve this, we will develop two optimal control problems, each using a distinct control strategy. The first strategy focuses on the effect of treatment for infected individuals, aiming to find the optimal treatment rate that reduces infection within the population. In the second strategy, we adjust the model to incorporate non-pharmaceutical interventions (i.e., self-precautionary measures and government-provided resources) along with treatment to assess their impact on preventing disease transmission.

The format of this manuscript is as follows: We explore the development of the influenza-corona co-infection model (Section 2). The essential characteristics of the solution are discussed, including the presence of uniqueness and positive bounded solutions (Section 3). We analyze the equilibrium points and the reproduction number ($\mathscr{R}_0$) (Section 4). Specifically, we explore the asymptotic stability of the disease-free equilibrium (DFE) and the endemic equilibrium (EE) points at the local and global levels. A sensitivity analysis of the reproduction number with respect to different parameters is included (Section 5). The study discusses several controls and presents their effects at various control levels and optimal control strategies including numerical simulation (Section 6). Numerical simulations are also included in this section to further highlight the findings. Finally, we provide a concise summary of the manuscript's key findings (Section 7).

2 Mathematical Model

We divide the total population, denoted as $N(t)$, into eight mutually distinct and time-dependent sub-classes or compartments, which we refer to as follows: susceptible $S(t)$, exposed $E(t)$, influenza-infectious $I_I(t)$, corona-infectious $I_C(t)$, influenza-corona infectious $I_{IC}(t)$, under treatment $T(t)$, hospitalized $H(t)$, and those who have recovered or have been removed from the population $R(t)$. The susceptible population $S(t)$ comprises individuals who are at risk of contracting influenza and corona infections following interactions with infectious individuals carrying either influenza, corona, or both viruses. After such interactions, a portion of the susceptible population transitions to the exposed state $E(t)$, making them vulnerable to coronavirus, influenza, or co-infection with both viruses. Following an incubation period of 2 to 5 days for influenza and 2 to 14 days for corona, those in the exposed category progress to become influenza-infectious $I_I(t)$, corona-infectious $I_C(t)$, or influenza-corona

co-infectious $I_{IC}(t)$. Individuals who are currently infected and receiving medical treatment in any form are placed in the treatment compartment $T(t)$. Patients with severe conditions, such as those requiring oxygen beds, are considered for hospitalization $H(t)$. Eventually, individuals who have successfully recovered from the diseases are categorized to move in the $R(t)$ compartment. The total population $N(t)$ can be written as:

$$N(t) = S(t) + E(t) + I_I(t) + I_C(t) + I_{IC}(t) + T(t) + H(t) + R(t), \tag{1}$$

and flow of co-infection through compartments is shown in Fig. 1. The transmission and translation rates ($\alpha's$, $\beta's$, and $\gamma's$, etc.) along with their complete description are given below:

- Π : Birth/Recruitment rate of susceptible population.
- α_1 : Transmission rate of influenza infection.
- α_2 : Transmission rate of corona infection.
- α_3 : Transmission rate of influenza-corona co-infection.
- β_1 : Translation rate of influenza exposed to influenza infectious.
- β_2 : Translation rate of corona exposed to corona infectious.
- β_3 : Translation rate of influenza-corona exposed to influenza-corona infectious.
- γ_1 : Translation rate of influenza infectious to influenza-corona infectious.
- γ_2 : Treatment rate of influenza infectious.
- γ_3 : Recovery rate of influenza infectious.
- τ_1 : Translation rate of corona infectious to influenza-corona infectious.
- τ_2 : Treatment rate of corona infectious.
- τ_3 : Recovery rate of corona infectious.
- δ_1 : Treatment rate of influenza-corona infectious.
- δ_2 : Recovery rate of influenza-corona infectious.
- ϕ_1 : Hospitalization rate of under-treatment patients.
- ϕ_2 : Recovery rate of under-treatment patients.
- ϕ_3 : Recovery rate of hospitalized patients.
- μ : Natural death rate.
- d_1 : Death rate due to influenza disease.
- d_2 : Death rate due to corona disease.
- d_3 : Death rate due to influenza-corona disease.
- d_4 : Death rate due to disease in under-treatment patients.
- d_5 : Death rate due to disease in hospitalized patients.

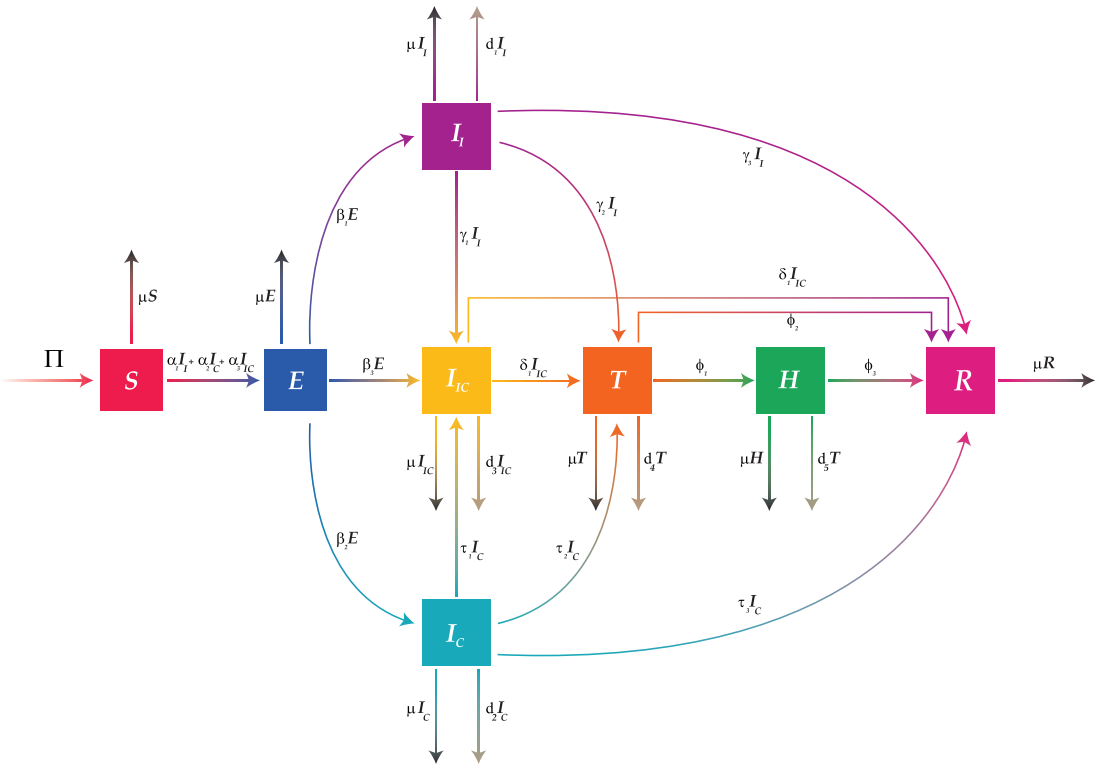

Figure 1: Flow diagram of the proposed influenza-corona co-infection model (Eq. (2))

We model the transmission of influenza-corona co-infection by the following system of non-linear differential equations.

$$\frac{dS}{dt} = \Pi - (\alpha_1 I_I + \alpha_2 I_C + \alpha_3 I_{IC})S - \mu S, \tag{2a}$$

$$\frac{dE}{dt} = (\alpha_1 I_I + \alpha_2 I_C + \alpha_3 I_{IC})S - (\beta_1 + \beta_2 + \beta_3 + \mu)E, \tag{2b}$$

$$\frac{dI_I}{dt} = \beta_1 E - (\gamma_1 + \gamma_2 + \gamma_3 + \mu + d_1)I_I, \tag{2c}$$

$$\frac{dI_C}{dt} = \beta_2 E - (\tau_1 + \tau_2 + \tau_c + \mu + d_2)I_C, \tag{2d}$$

$$\frac{dI_{IC}}{dt} = \beta_3 E + \gamma_1 I_I + \tau_1 I_C - (\delta_1 + \delta_2 + \mu + d_3)I_{IC}, \tag{2e}$$

$$\frac{dT}{dt} = \gamma_2 I_I + \tau_2 I_C + \delta_1 I_{IC} - (\phi_1 + \phi_2 + \mu + d_4)T, \tag{2f}$$

$$\frac{dH}{dt} = \phi_1 T - (\phi_3 + \mu + d_5)H, \tag{2g}$$

$$\frac{dR}{dt} = \gamma_3 I_I + \tau_c I_C + \delta_2 I_{IC} + \phi_2 T + \phi_3 H - \mu R, \tag{2h}$$

with the non-negative initial conditions:

$$S(0) > 0,\ E(0) \geq 0,\ I_I(0) \geq 0,\ I_C(0) \geq 0,\ I_{IC}(0) \geq 0,\ T(0) \geq 0,\ H(0) \geq 0,\ R(0) \geq 0. \tag{2i}$$

The above autonomous system can be written in compact form as:

$$\frac{dy}{dt} = F(y(t)), \qquad y(0) = y_0, \quad 0 < t < \mathbb{T} < +\infty, \tag{3}$$

where $y : [0, \mathbb{T}] \to \mathbb{R}^8_+$ and $F : \mathbb{R}^8_+ \to \mathbb{R}^8_+$ are vector valued functions such that

$$y(t) = \begin{pmatrix} S(t) \\ E(t) \\ I_I(t) \\ I_C(t) \\ I_{IC}(t) \\ T(t) \\ H(t) \\ R(t) \end{pmatrix}, \qquad y(0) = \begin{pmatrix} S(0) \\ E(0) \\ I_I(0) \\ I_C(0) \\ I_{IC}(0) \\ T(0) \\ H(0) \\ R(0) \end{pmatrix},$$

and

$$F(y) = \begin{pmatrix} F_1 \\ F_2 \\ F_3 \\ F_4 \\ F_5 \\ F_6 \\ F_7 \\ F_8 \end{pmatrix} = \begin{pmatrix} \Pi - (\alpha_1 I_I + \alpha_2 I_C + \alpha_3 I_{IC})S - \mu S \\ (\alpha_1 I_I + \alpha_2 I_C + \alpha_3 I_{IC})S - (\beta_1 + \beta_2 + \beta_3 + \mu)E \\ \beta_1 E - (\gamma_1 + \gamma_2 + \gamma_3 + \mu + d_1)I_I \\ \beta_2 E - (\tau_1 + \tau_2 + \tau_c + \mu + d_2)I_C \\ \beta_3 E + \gamma_1 I_I + \tau_1 I_C - (\delta_1 + \delta_2 + \mu + d_3)I_{IC} \\ \gamma_2 I_I + \tau_2 I_C + \delta_1 I_{IC} - (\phi_1 + \phi_2 + \mu + d_4)T \\ \phi_1 T - (\phi_3 + \mu + d_5)H \\ \gamma_3 I_I + \tau_c I_C + \delta_2 I_{IC} + \phi_2 T + \phi_3 H - \mu R \end{pmatrix},$$

respectively.

3 Theoretical Properties and Proofs

The fundamental characteristics of the proposed mathematical model, such as the existence of a unique solution and a positive, bounded solution in a feasible region is demonstrated in this section.

Theorem 3.1. The co-infection model (Eq. (2)) has a bounded solution, $y(t) = \big(S(t), E(t), I_I(t), I_C(t), I_{IC}(t), T(t), H(t), R(t)\big)$.

Proof. By differentiating Eq. (1) w.r.t time t and then adding right hand side of ODEs of the system (Eq. (2)), we get an equation of the form

$$\frac{dN}{dt} = \Pi - \mu N - (d_1 I_I + d_2 I_C + d_3 I_{IC} + d_4 T + d_5 H), \tag{4}$$

with

$$N_0 = N(0) = S(0) + E(0) + I_I(0) + I_C(0) + I_{IC}(0) + T(0) + H(0) + R(0) \leq \frac{\Pi}{\mu}. \tag{5}$$

Since, $d_1 I_I + d_2 I_C + d_3 I_{IC} + d_4 T + d_5 H \geq 0$, hence Eq. (4) can be written as:

$$\frac{dN}{dt} \leq \Pi - \mu N. \tag{6}$$

By using the properties of the Laplace transformation and partial fraction on inequality (6), we get

$$\mathbb{L}\{\frac{dN(t)}{dt}\} \leq \mathbb{L}\{\Pi\} - \mu \mathbb{L}\{N(t)\}, \tag{7}$$

$$N(s) \leq \frac{\Pi}{\mu s} - \frac{\Pi}{\mu(s+\mu)} + \frac{N_0}{(s+\mu)}. \tag{8}$$

The Laplace inverse transformation yield us

$$\mathbb{L}^{-1}\{N(s)\} \leq \mathbb{L}^{-1}\{\frac{\Pi}{\mu s}\} - \mathbb{L}^{-1}\{\frac{\Pi}{\mu(s+\mu)}\} + \mathbb{L}^{-1}\{\frac{N_0}{(s+\mu)}\}, \tag{9}$$

$$N(t) \leq \frac{\Pi}{\mu} - e^{-\mu t}(\frac{\Pi}{\mu} - N_0). \tag{10}$$

Thus,

$$\lim_{t\to\infty} N(t) \leq \frac{\Pi}{\mu}. \tag{11}$$

Thus, $y(t)$ is a bounded solution $\forall\ t \geq 0$. ■

Theorem 3.2. With the positive initial conditions, the co-infection model (Eq. (2)) has a positive solution $y(t) = \big(S(t), E(t), I_I(t), I_C(t), I_{IC}(t), T(t), H(t), R(t)\big)$ for all $t \geq 0$.

Proof. Since, $y(0)$ represent the total population at $t = 0$, hence, $y(0) \geq 0$. Let us prove the positivity of one state variable and the left can be proved similarly. Let us take Eq. (2a)

$$\frac{dS}{dt} = \Pi - (\alpha_1 I_I + \alpha_2 I_C + \alpha_3 I_{IC} + \mu)S.$$

As we already proved all the state variables are bounded by $\frac{\Pi}{\mu}$, therefore, $\exists\ \chi > 0$ such that

$$\chi = sup\ [\alpha_1 I_I + \alpha_2 I_C + \alpha_3 I_{IC} + \mu].$$

Thus,

$$\frac{dS}{dt} \geq \Pi - \chi S(t).$$

Applying the Laplace transformation gives

$$\mathbb{L}\{\frac{dS}{dt}\} \geq \mathbb{L}\{\Pi - \chi S(t)\},$$

$$S(s) \geq \frac{\Pi}{s(s+\chi)} + \frac{S_0}{(s+\chi)}.$$

Now, using the inverse Laplace transformation

$$\mathbb{L}^{-1}\{S(s)\} \geq \mathbb{L}^{-1}\{\frac{\Pi}{s(s+\chi)}\} + \mathbb{L}^{-1}\{\frac{S_0}{(s+\chi)}\},$$

$$S(t) \geq \frac{\Pi}{\chi} - \frac{\Pi}{\chi}e^{-\chi t} + S_0 e^{-\chi t}. \tag{12}$$

Since $0 \leq e^{-\chi t} \leq 1, and\ S_0 e^{-\chi t} > 0$. Thus, it is self evident that S(t) $\geq 0\ \forall\ t \geq 0$. Furthermore, we can verify this for other state variables. Thus, the feasible region of the proposed influenza-corona co-infection model (Eq. (2)) is given by

$$\Psi = \left\{ \left(S(t), E(t), I_I(t), I_C(t), I_{IC}(t), T(t), H(t), R(t) \right) \in R_+^8 : 0 < N(t) \leq \frac{\Pi}{\mu}, \forall t \geq 0 \right\}. \tag{13}$$

■

Before proving the existence and uniqueness properties of the solution of the proposed model, we define following fundamental theorems:

Theorem 3.3. [27] Suppose $\mathscr{S} = \{(t, u_1, u_2, u_3, \ldots, u_m) | a \leq t \leq b, -\infty < u_i < \infty$, for each $i = 1, 2, 3 \ldots, m\}$, and let $f_i(t, u_1, u_2, u_3, \ldots, u_m)$ for each $i = 1, 2, 3 \ldots, m$ be continuous on $\mathscr{S}$ and satisfies a Lipchitz condition there. The system of first order differential equations $\frac{du_i}{dt} = f_i(t, u_i)$ with $u_i(a) = \omega_i$ for each $i = 1, 2, 3 \ldots, m$, has a unique solution for all $a \leq t \leq b$.

Theorem 3.4. The model (Eq. (3)) has a unique solution on $[0, \mathbb{T}]$ if $F(y(t))$ is Lipschitz continuous on $[0, \mathbb{T}]$.

Proof. Since, all the state variables are assumed to be continuously differentiable on $[0, \mathbb{T}]$, therefore, $F(y(t))$ and first partial derivatives of $F(y(t))$ are also continuous on $[0, \mathbb{T}]$. Theorems 3.1 and 3.2 guarantee that $F(y(t))$ is bounded on $[0, \mathbb{T}]$, i.e., $0 < F(y(t)) \leq \frac{\Pi}{\mu}$. Thus, if the partial derivatives of the $F(y(t))$ are bounded, then Theorem 3.3 implies existence of a unique solution to the problem (Eq. (2)).

To prove Lipschitz condition, we need to prove that $F(y(t))$ has partial derivatives with respect to all state variables and are bounded.

$$|\frac{\partial F_1}{\partial S}| = |-(\alpha_1 I_I + \alpha_2 I_C + \alpha_3 I_{IC} + \mu)| \leq \frac{\Pi}{\mu} < \infty,\ |\frac{\partial F_1}{\partial E}| = 0,\ |\frac{\partial F_1}{\partial I_I}| = |-\alpha_1 S| \leq \frac{\Pi}{\mu},$$

$$|\frac{\partial F_1}{\partial I_C}| = |-\alpha_2 S| \leq \frac{\Pi}{\mu},\ |\frac{\partial F_1}{\partial I_{IC}}| = |-\alpha_3 S| \leq \frac{\Pi}{\mu},\ |\frac{\partial F_1}{\partial T}| = |\frac{\partial F_1}{\partial H}| = |\frac{\partial F_1}{\partial R}| = 0,$$

$$|\frac{\partial F_2}{\partial S}| = |\alpha_1 I_I + \alpha_2 I_C + \alpha_3 I_{IC}| \leq \frac{\Pi}{\mu} < \infty,\ |\frac{\partial F_2}{\partial E}| = |\beta_1 + \beta_2 + \beta_3 + \mu|,\ |\frac{\partial F_2}{\partial I_I}| = |\alpha_1 S| \leq \frac{\Pi}{\mu},$$

$$|\frac{\partial F_2}{\partial I_C}| = |\alpha_2 S| \leq \frac{\Pi}{\mu},\ |\frac{\partial F_2}{\partial I_{IC}}| = |\alpha_3 S| \leq \frac{\Pi}{\mu},\ |\frac{\partial F_2}{\partial T}| = |\frac{\partial F_2}{\partial H}| = |\frac{\partial F_2}{\partial R}| = 0,\ |\frac{\partial F_3}{\partial S}| = 0,\ |\frac{\partial F_3}{\partial E}| = \beta_1,$$

$$|\frac{\partial F_3}{\partial I_I}| = |(\gamma_1 + \gamma_2 + \gamma_3 + \mu + d_1)|,\ |\frac{\partial F_3}{\partial I_C}| = |\frac{\partial F_3}{\partial I_{IC}}| = |\frac{\partial F_3}{\partial T}| = |\frac{\partial F_3}{\partial H}| = |\frac{\partial F_3}{\partial R}| = 0,\ |\frac{\partial F_4}{\partial S}| = 0,$$

$$|\frac{\partial F_4}{\partial E}| = \beta_2,\ |\frac{\partial F_4}{\partial I_I}| = 0,\ |\frac{\partial F_4}{\partial I_C}| = |-(\tau_1 + \tau_2 + \tau_c + \mu + d_2)|,\ |\frac{\partial F_4}{\partial I_{IC}}| = |\frac{\partial F_4}{\partial T}| = |\frac{\partial F_4}{\partial H}| = |\frac{\partial F_4}{\partial R}| = 0,$$

$$|\frac{\partial F_5}{\partial S}| = 0,\ |\frac{\partial F_5}{\partial E}| = \beta_3,\ |\frac{\partial F_5}{\partial I_I}| = \gamma_1,\ |\frac{\partial F_5}{\partial I_C}| = |\tau_1|,\ |\frac{\partial F_5}{\partial I_{IC}}| = |-(\delta_1 + \delta_2 + \mu + d_3)|,$$

$$|\frac{\partial F_5}{\partial T}| = |\frac{\partial F_5}{\partial H}| = |\frac{\partial F_5}{\partial R}| = 0,\ |\frac{\partial F_6}{\partial S}| = |\frac{\partial F_6}{\partial E}| = 0,\ |\frac{\partial F_6}{\partial I_I}| = |\gamma_2|,\ |\frac{\partial F_6}{\partial I_C}| = |\tau_2|,\ |\frac{\partial F_6}{\partial I_{IC}}| = |\delta_1|,$$

$$|\frac{\partial F_6}{\partial T}| = |-(\phi_1 + \phi_2 + \mu + d_4)|,\ |\frac{\partial F_6}{\partial H}| = |\frac{\partial F_6}{\partial R}| = 0,\ |\frac{\partial F_7}{\partial S}| = |\frac{\partial F_7}{\partial E}| = |\frac{\partial F_7}{\partial I_I}| = |\frac{\partial F_7}{\partial I_C}| = |\frac{\partial F_7}{\partial I_{IC}}| = 0,$$

$$|\frac{\partial F_7}{\partial T}| = |\phi_1|,\ |\frac{\partial F_7}{\partial H}| = |-(\phi_3 + \mu + d_5)|,\ |\frac{\partial F_7}{\partial R}| = 0,\ |\frac{\partial F_8}{\partial S}| = 0|\frac{\partial F_8}{\partial E}| = 0,\ |\frac{\partial F_8}{\partial I_I}| = |\gamma_3|,$$

$$|\frac{\partial F_8}{\partial I_C}| = |\tau_c|,\ |\frac{\partial F_8}{\partial I_{IC}}| = |\delta_2|,\ |\frac{\partial F_8}{\partial T}| = |\phi_2|,\ |\frac{\partial F_8}{\partial H}| = |\phi_3|,\ |\frac{\partial F_8}{\partial R}| = |-\mu|.$$

It is clear that all the partial derivatives, $\frac{\partial F_i}{\partial y_j}$, $i,j = 1,2,3,\ldots,8$, exist and are bounded on $[0,\mathbb{T}]$. Thus, Theorem 3.3 guarantees that the model (Eq. (3)) has a unique solution. ■

Thus, we have proved that the proposed model (Eq. (2)) has a unique, positive, and bounded solution (Fig. 2).

4 Equilibrium Points and Associated Properties

In this section, we determine the important equilibrium points and the properties associated with these equilibrium points. Specifically, we drive the reproduction number $\mathscr{R}_0$ and perform stability analysis of the system at the equilibrium points. All the analytical results of stability analysis are validated through numerical simulations and given at the end of each section (Figs. 3 and 4).

4.1 Equilibrium Points and Reproduction Number

To find equilibrium points, we consider the rate of change of all the state variables equal to zero, i.e., $\frac{dS}{dt} = \frac{dE}{dt} = \frac{dI_I}{dt} = \frac{dI_C}{dt} = \frac{dI_{IC}}{dt} = \frac{dT}{dt} = \frac{dH}{dt} = \frac{dR}{dt} = 0$. There are two main equilibrium points that exist for an epidemic model, DFE point and EE point. To find DFE point of an epidemic model, we assume that there is no infection present, i.e., $E = I_C = I_I = I_{IC} = 0$. Thus, the DFE point of the

corona-influenza co-infection model (Eq. (2)) is given as:

$$P^* = (S^*, E^*, I_C{}^*,\ I_I{}^*,\ I_{IC}{}^*,\ T^*,\ H^*,\ R^*) = \left(\frac{\Pi}{\mu},\ 0,\ 0,\ 0,\ 0,\ 0,\ 0,\ 0\right). \tag{14}$$

A critical epidemiological metric that quantifies the average number of secondary infections produced by a single infectious person in a fully susceptible (disease free) population is the reproduction number $\mathscr{R}_0$. The $\mathscr{R}_0$ can be computed mathematically using the next-generation matrix method [28–30]. To calculate $\mathscr{R}_0$, we sub-divide infection carrier compartments into $\mathscr{F}$ and $\mathscr{G}$:

$$\mathscr{F} = \begin{pmatrix} (\alpha_1 I_I + \alpha_2 I_C + \alpha_3 I_{IC})S \\ 0 \\ 0 \\ 0 \end{pmatrix}, \qquad \mathscr{G} = \begin{pmatrix} k_1 E \\ -\beta_1 E + k_2 I_I \\ -\beta_2 E + k_3 I_C \\ -\beta_3 E - \gamma_1 I_I - \tau_1 I_C + k_4 I_{IC} \end{pmatrix},$$

where, $k_1 = \beta_1+\beta_2+\beta_3+\mu$, $k_2 = \gamma_1+\gamma_2+\gamma_3+\mu+d_1$, $k_3 = \tau_1+\tau_2+\tau_c+\mu+d_2$, and $k_4 = \delta_1+\delta_2+\mu+d_3$.

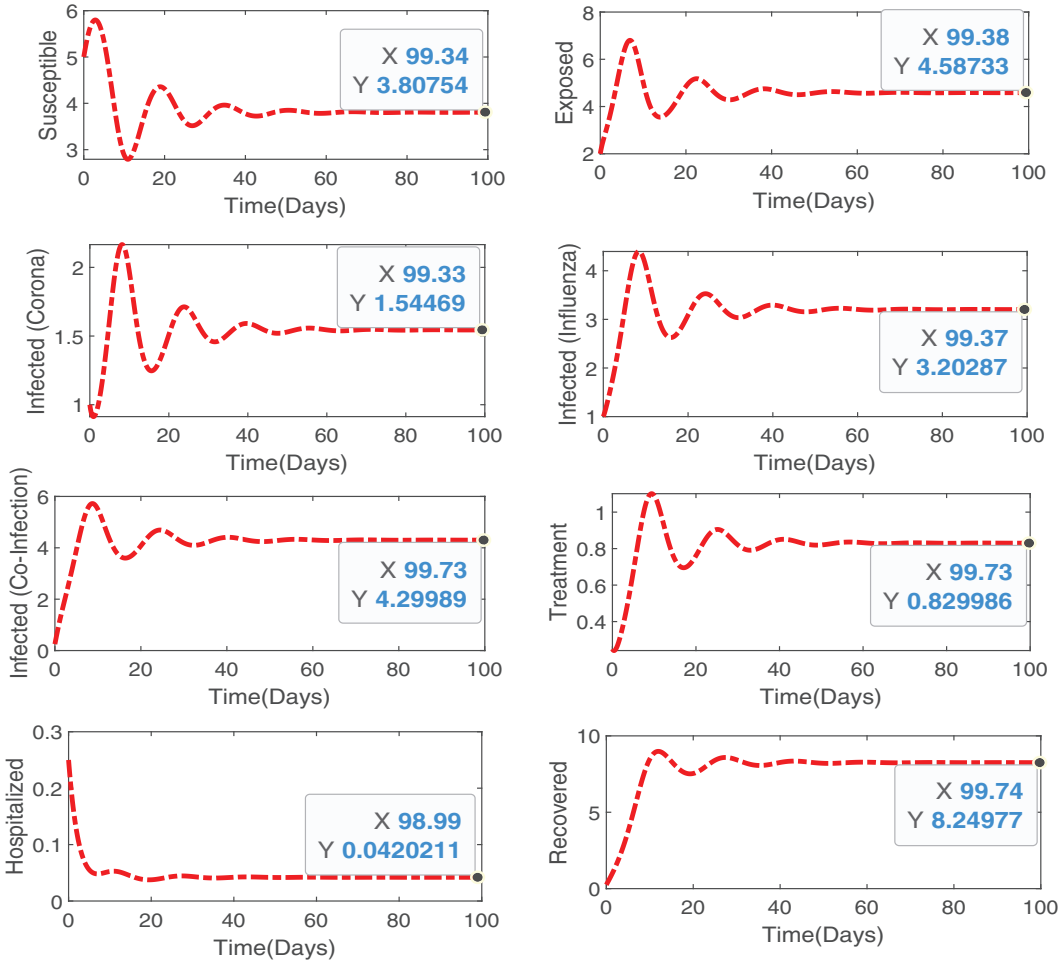

Figure 2: Numerical simulations illustrating theoretical results proved analytically, that our proposed model is bounded and positive within a feasible region and has a unique solution

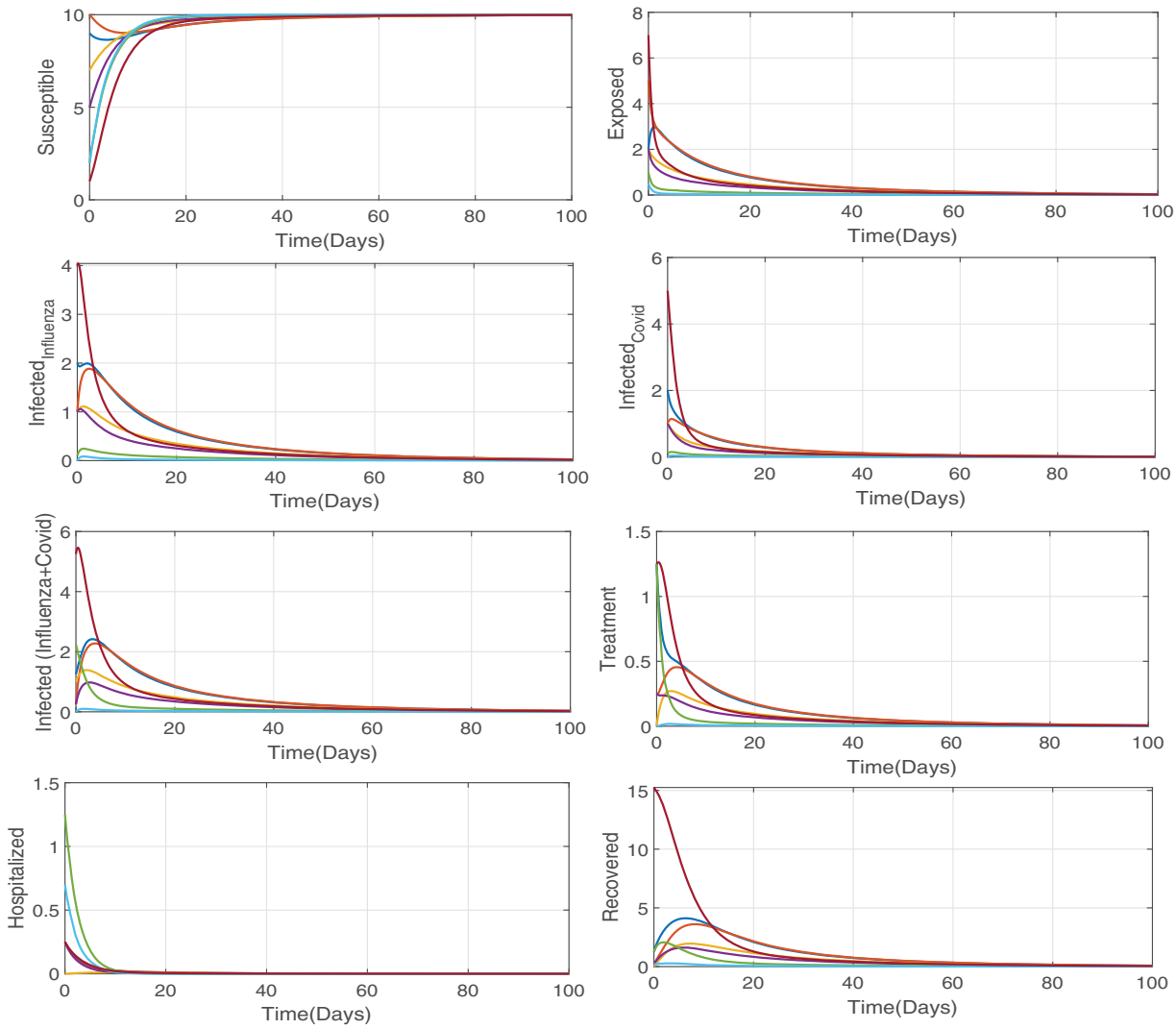

Figure 3: Numerical simulation illustrating the our proposed model (Eq. (2)) is stable at disease free equilibrium point when $\mathscr{R}_0 < 1$ (proved in Theorem 4.2). We numerically solve the system with different initial values, and all the solution curves approaches same point which is the disease free equilibrium point

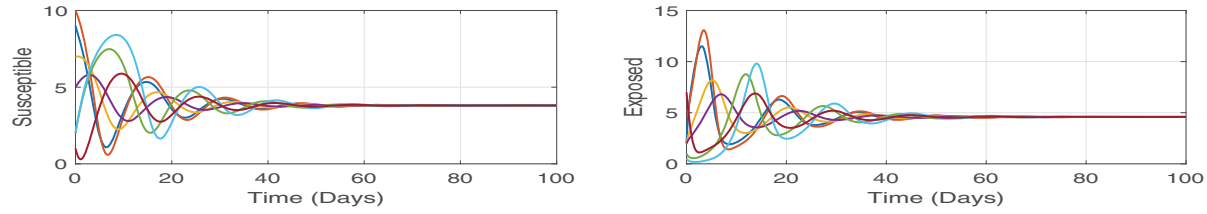

Figure 4: (Continued)

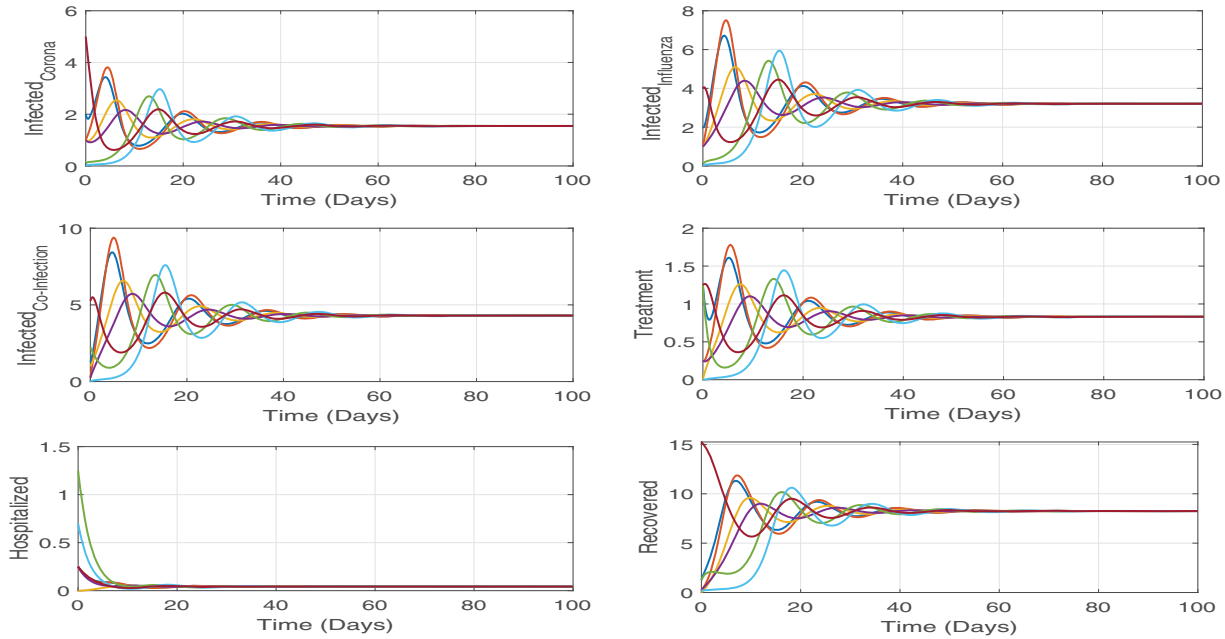

Figure 4: We numerically solve the system by using different initial values, but all the solutions approach same point which is the endemic point. These simulations demonstrate the state theorem (Theorem 4.4) that the proposed model (Eq. (2)) is stable at endemic equilibrium point (P^{**})

The Jacobian of the matrices $\mathscr{F}$ and $\mathscr{G}$ evaluated at DFE point P^* are given as:

$$\mathbb{F} = \begin{pmatrix} 0 & \frac{\alpha_1\Pi}{\mu} & \frac{\alpha_2\Pi}{\mu} & \frac{\alpha_3\Pi}{\mu} \\ 0 & 0 & 0 & 0 \\ 0 & 0 & 0 & 0 \\ 0 & 0 & 0 & 0 \end{pmatrix}, \qquad \mathbb{G} = \begin{pmatrix} k_1 & 0 & 0 & 0 \\ -\beta_1 & k_2 & 0 & 0 \\ -\beta_2 & 0 & k_3 & 0 \\ -\beta_3 & -\gamma_1 & -\tau_1 & k_4 \end{pmatrix}.$$

Thus, the spectral radius of $\mathbb{F}\mathbb{G}^{-1} = \mathscr{R}_0 = \mathscr{R}_I + \mathscr{R}_C + \mathscr{R}_{IC}$,

where

$$\mathscr{R}_I = \frac{\Pi\alpha_1\beta_1}{\mu k_1 k_2}, \mathscr{R}_C = \frac{\Pi\alpha_2\beta_2}{\mu k_1 k_3}, \text{ and } \mathscr{R}_{IC} = \frac{\alpha_3\Pi}{\mu}\left(\frac{\beta_3}{k_1k_4} + \frac{\beta_1\gamma_1}{k_1k_2k_4} + \frac{\beta_2\tau_1}{k_1k_2k_3}\right).$$

Here $\mathscr{R}_I$, $\mathscr{R}_C$, and $\mathscr{R}_{IC}$ represent the reproduction number of influenza, corona and influenza-corona co-infection, respectively. Thus, the reproduction number of the whole model (Eq. (2)) is given as:

$$\mathscr{R}_0 = \frac{\Pi}{\mu}\left[\frac{\alpha_1\beta_1k_3k_4 + \alpha_2\beta_2k_2k_4 + \alpha_3\beta_3k_2k_3 + \alpha_3\gamma_1\beta_1k_3 + \alpha_3\tau_1\beta_2k_2}{k_1k_2k_3k_4}\right]. \tag{15}$$

Local Stability at DFE

Theorem 4.1. The proposed model (Eq. (2)) is locally asymptotically stable (LAS) at the disease free equilibrium point P^* if $\mathscr{R}_0 < 1$ and unstable for $\mathscr{R}_0 > 1$.

Proof. This theorem can be proved by using the Jacobian matrix approach. For this purpose, we need to find Jacobian matrix at DFE point, i.e.,

$$J(P^*) = \begin{pmatrix} -\mu & 0 & -\frac{\alpha_1\Pi}{\mu} & -\frac{\alpha_2\Pi}{\mu} & -\frac{\alpha_3\Pi}{\mu} & 0 & 0 & 0 \\ 0 & -k_1 & \frac{\alpha_1\Pi}{\mu} & \frac{\alpha_2\Pi}{\mu} & \frac{\alpha_3\Pi}{\mu} & 0 & 0 & 0 \\ 0 & \beta_1 & -k_2 & 0 & 0 & 0 & 0 & 0 \\ 0 & \beta_2 & 0 & -k_3 & 0 & 0 & 0 & 0 \\ 0 & \beta_3 & \gamma_1 & \tau_1 & -k_4 & 0 & 0 & 0 \\ 0 & 0 & \gamma_2 & \tau_2 & \delta_1 & -k_5 & 0 & 0 \\ 0 & 0 & 0 & 0 & 0 & \phi_1 & -k_6 & 0 \\ 0 & 0 & \gamma_3 & \tau_c & \delta_2 & \phi_2 & \phi_3 & -\mu \end{pmatrix}. \tag{16}$$

As we know that, a system is said to be stable at an equilibrium if all the eigenvalues are negative at this equilibrium point and unstable otherwise. Therefore, we calculate the eigenvalues of the above matrix with the help of Maple software:

$$\lambda_1^* = -\mu, \tag{17a}$$

$$\lambda_2^* = -\mu, \tag{17b}$$

$$\lambda_3^* = -k_6, \tag{17c}$$

$$\lambda_4^* = -k_5, \tag{17d}$$

$$\lambda_5^* = -k_1, \tag{17e}$$

$$\lambda_6^* = -k_2\left(1 - \frac{\beta_1\alpha_1\Pi}{\mu k_1 k_2}\right), \tag{17f}$$

$$\lambda_7^* = \left[\frac{(1-\mathscr{R}_0) + (\alpha_3\beta_3k_2k_3 + \alpha_3\beta_3k_2k_3 + \alpha_3\gamma_1\beta_1k_3 + \alpha_3\tau_1\beta_2k_2)}{k_1k_4\mu\lambda_6^*}\right], \tag{17g}$$

$$\lambda_8^* = -\frac{[1-\mathscr{R}_0]}{k_1\mu\lambda_6^*\lambda_7^*}. \tag{17h}$$

Since all the eigenvalues are negatives when $\mathscr{R}_0 < 1$, $\frac{\beta_1\alpha_1\Pi}{\mu k_1 k_2} < 1$ (true) and at least Eq. (17h) is positive otherwise. Thus, our proposed co-infection model (Eq. (2)) is locally asymptotically stable at DFE point (Eq. (14)). ■

4.2 Global Stability

In order to show that the DFE point P^* is globally stable, we use the approach given by Castillo-Chavez [31].

Theorem 4.2. The disease free equilibrium (DFE) point P^* of the model (Eq. (2)) is globally asymptotically stable (GAS) if $\mathscr{R}_0 < 1$ and the conditions ($\mathscr{H}1$) and ($\mathscr{H}2$) are fulfilled:

$$(\mathscr{H}1) \quad \frac{d\mathbb{X}}{dt} = \mathbb{K}(\mathbb{X}, 0) = 0, \ \mathbb{X}^0 \text{ is } GAS,$$

$$(\mathscr{H}2) \quad \frac{d\mathbb{Y}}{dt} = \mathbb{N}(\mathbb{X}, \mathbb{Y}) = \mathbb{B}\mathbb{Y} - \bar{\mathbb{N}}(\mathbb{X}, \mathbb{Y}),$$

where $\bar{\mathbb{N}}(\mathbb{X}, \mathbb{Y}) \geq 0 \ \forall \ t \geq 0$ and $\mathbb{B} = D_{\mathbb{Y}}\mathbb{N}(\mathbb{X}^0, 0)$ is an M-matrix.

Proof. Let $\mathbb{X} = (S)$ represents non-infectious class and $\mathbb{Y} = (E, I_I, I_C, I_{IC}, T)$ represent infectious classes, and $P^* = (\mathbb{X}^*, 0)$ is the DFE point. So,

$$\frac{d\mathbb{X}}{dt} = \mathbb{K}(\mathbb{X}, \mathbb{Y}) = \Pi - (\alpha_1 I_I + \alpha_2 I_C + \alpha_3 I_{IC})S - \mu S. \tag{18}$$

If $\mathbb{X} = \mathbb{X}^*$, then $\mathbb{K}(\mathbb{X}, 0) = 0$, i.e.,

$$\frac{d\mathbb{X}}{dt} = \Pi - \mu S^* = 0. \tag{19}$$

From Eq. (19), as $t \to \infty$, $\mathbb{X} \to \mathbb{X}^*$. Therefore, $\mathbb{X}^*$ is GAS. Now,

$$\frac{d\mathbb{Y}}{dt} = \mathbb{B}\mathbb{Y} - \bar{\mathbb{N}}(\mathbb{X}, \mathbb{Y}) = \begin{bmatrix} -k_1 & \frac{\alpha_1\Pi}{\mu} & \frac{\alpha_2\Pi}{\mu} & \frac{\alpha_3\Pi}{\mu} & 0 & 0 \\ \beta_1 & -k_2 & 0 & 0 & 0 & 0 \\ \beta_2 & 0 & -k_3 & 0 & 0 & 0 \\ \beta_3 & \gamma_1 & \tau_1 & -k_4 & 0 & 0 \\ 0 & \gamma_2 & \tau_2 & \delta_1 & -k_5 & 0 \\ 0 & 0 & 0 & 0 & \phi_1 & -k_6 \end{bmatrix} \begin{bmatrix} E \\ I_I \\ I_C \\ I_{IC} \\ T \\ H \end{bmatrix} - \begin{bmatrix} \kappa \\ 0 \\ 0 \\ 0 \\ 0 \\ 0 \end{bmatrix}, \tag{20}$$

where

$$\mathbb{B} = \begin{bmatrix} -k_1 & \frac{\alpha_1\Pi}{\mu} & \frac{\alpha_2\Pi}{\mu} & \frac{\alpha_3\Pi}{\mu} & 0 & 0 \\ \beta_1 & -k_2 & 0 & 0 & 0 & 0 \\ \beta_2 & 0 & -k_3 & 0 & 0 & 0 \\ \beta_3 & \gamma_1 & \tau_1 & -k_4 & 0 & 0 \\ 0 & \gamma_2 & \tau_2 & \delta_1 & -k_5 & 0 \\ 0 & 0 & 0 & 0 & \phi_1 & -k_6 \end{bmatrix}, \quad \mathbb{Y} = \begin{bmatrix} E \\ I_I \\ I_C \\ I_{IC} \\ T \\ H \end{bmatrix}, \quad \bar{\mathbb{N}}(\mathbb{X}, \mathbb{Y}) = \begin{bmatrix} \kappa \\ 0 \\ 0 \\ 0 \\ 0 \\ 0 \end{bmatrix},$$

and $\kappa = (\alpha_1 I_I + \alpha_2 I_C + \alpha_3 I_{IC})(S^* - S)$.

It is evident that $\mathbb{B}$ is an M-matrix. Since at the DFE point $N = S^*$, matrix $\bar{\mathbb{N}}(\mathbb{X}, \mathbb{Y}) \geq 0$. So, the DFE point P^* is GAS. ■

4.2.1 Endemic Equilibrium Point

To find endemic equilibrium point (P^{**}), we set $E \neq 0, I_I \neq 0, I_C \neq 0$ and $I_{IC} \neq 0$ in steady state equation of model (Eq. (2)).

$$P^{**} = (S^{**}, E^{**}, {I_C}^{**}, {I_I}^{**}, {I_{IC}}^{**}, T^{**}, H^{**}, R^{**}), \tag{21}$$

where

$$S^{**} = \frac{\Pi}{\mu}\frac{k_1}{\mathscr{R}_0}, E^{**} = \Pi\left(\frac{\mathscr{R}_0 - k_1}{k_1\mathscr{R}_0}\right), {I_I}^{**} = \frac{\beta_1}{k_2}E^{**}, {I_C}^{**} = \frac{\beta_2}{k_3}E^{**}, {I_{IC}}^{**} = \frac{\beta_3 k_2 k_3 + \gamma_1\beta_1 k_3 + \tau_1\beta_2 k_2}{k_2 k_3 k_4}E^{**},$$

$$T^{**} = \frac{\gamma_2 {I_I}^{**} + \tau_2 {I_C}^{**} + \delta_1 {I_{IC}}^{**}}{k_5}, H^{**} = \frac{\phi_1 T^{**}}{k_6}, R^{**} = \frac{\gamma_3 {I_I}^{**} + \tau_c {I_C}^{**} + \delta_2 {I_{IC}}^{**} + \phi_2 T^{**} + \phi_3 H^{**}}{\mu}.$$

4.2.2 Local Stability at EE

Theorem 4.3. The Model (Eq. (2)) is locally asymptotically stable (LAS) at endemic equilibrium point P^{**} if $\mathscr{R}_0 > 1$ and is unstable for $\mathscr{R}_0 < 1$.

Proof. Now, we linearized the proposed model (Eq. (2)) at endemic equilibrium point (P^{**}), i.e.,

$$J(P^{**}) = \begin{pmatrix} -(\mu + \alpha_1 {I_I}^{**} + \alpha_2 {I_C}^{**} + \alpha_3 {I_{IC}}^{**}) & 0 & -\frac{\alpha_1}{\mathscr{R}_0} & -\frac{\alpha_2}{\mathscr{R}_0} & -\frac{\alpha_3}{\mathscr{R}_0} & 0 & 0 & 0 \\ \alpha_1 {I_I}^{**} + \alpha_2 {I_C}^{**} + \alpha_3 {I_{IC}}^{**} & -k_1 & \frac{\alpha_1}{\mathscr{R}_0} & \frac{\alpha_2}{\mathscr{R}_0} & \frac{\alpha_3}{\mathscr{R}_0} & 0 & 0 & 0 \\ 0 & \beta_1 & -k_2 & 0 & 0 & 0 & 0 & 0 \\ 0 & \beta_1 & 0 & -k_3 & 0 & 0 & 0 & 0 \\ 0 & \beta_3 & \gamma_1 & \tau_1 & -k_4 & 0 & 0 & 0 \\ 0 & 0 & \gamma_2 & \tau_2 & \delta_1 & -k_5 & 0 & 0 \\ 0 & 0 & 0 & 0 & 0 & \phi_1 & -k_6 & 0 \\ 0 & 0 & \gamma_3 & \tau_c & \delta_2 & \phi_2 & \phi_3 & -\mu \end{pmatrix}.$$

$$\lambda_1^{**} = -\mu, \tag{22a}$$

$$\lambda_2^{**} = -k_5, \tag{22b}$$

$$\lambda_3^{**} = -k_6, \tag{22c}$$

$$\lambda_4^{**} = -\mu\mathscr{R}_0, \tag{22d}$$

$$\lambda_5^{**} = -k_1, \tag{22e}$$

$$\lambda_6^{**} = -k_2\left(1 - \frac{\alpha_1\beta_1\Pi}{{\mathscr{R}_0}^2 k_1 k_2 \mu}\right), \tag{22f}$$

$$\lambda_7^{**} = -\frac{k_2 k_3}{\lambda_6^{**}\mathscr{R}_0}\left[1 - \mathscr{R}_0 - \frac{\alpha_3\beta_3 k_2 k_3 + \alpha_3\gamma_1\beta_1 k_3 + \alpha_3\tau_1\beta_2 k_2}{\mathscr{R}_0 k_1 k_2 k_3 k_4 \mu}\right], \tag{22g}$$

$$\lambda_8^{**} = -\left(\frac{k_2k_3k_4}{\lambda_6^{**}\lambda_7^{**}\mathscr{R}_0}\right)(\mathscr{R}_0 - 1)\,. \tag{22h}$$

Since all the eigenvalues are negative when $\mathscr{R}_0 > 1$, $\frac{\alpha_1\beta_1\Pi}{\mathscr{R}_0{}^2k_1k_2\mu} < 1$ (true) and unstable otherwise, the proposed co-infection model is LAS at EE point (P^{**}). ■

4.2.3 Global Stability at EE

Theorem 4.4. The endemic equilibrium (EE) point P^{**} of the model (Eq. (2)) is globally asymptotically stable (GAS) provided $\mathscr{R}_0 > 1$ and unstable when $\mathscr{R}_0 < 1$.

Proof. Let $\mathscr{L}$ be a Volterra-type Lyapunov function and defined as:

$$\begin{aligned}\mathscr{L}(S,E,I_I,I_C,I_{IC},T,H,R) = &\left[S - S^{**} - S^{**}\log\frac{S}{S^{**}}\right] + \left[E - E^{**} - E^{**}\log\frac{E}{E^{**}}\right]\\ &+ \left[I_I - I_I^{**} - I_I^{**}\log\frac{I_I}{I_I^{**}}\right] + \left[I_C - I_C^{**} - I_C^{**}\log\frac{I_C}{I_C^{**}}\right]\\ &+ \left[I_{IC} - I_{IC}^{**} - I_{IC}^{**}\log\frac{I_{IC}}{I_{IC}^{**}}\right] + \left[T - T^{**} - T^{**}\log\frac{T}{T^{**}}\right]\\ &+ \left[H - H^{**} - H^{**}\log\frac{H}{H^{**}}\right] + \left[R - R^{**} - R^{**}\log\frac{R}{R^{**}}\right].\end{aligned} \tag{23}$$

Taking the derivative of Eq. (23) w.r.t time t:

$$\begin{aligned}\frac{d\mathscr{L}}{dt} = &\left[\frac{S - S^{**}}{S}\right]\frac{dS}{dt} + \left[\frac{E - E^{**}}{E}\right]\frac{dE}{dt} + \left[\frac{I_I - I_I^{**}}{I_I}\right]\frac{dI_I}{dt} + \left[\frac{I_C - I_C^{**}}{I_C}\right]\frac{dI_C}{dt}\\ &+ \left[\frac{I_{IC} - I_{IC}^{**}}{I_{IC}}\right]\frac{dI_{IC}}{dt} + \left[\frac{T - T^{**}}{T}\right]\frac{dT}{dt} + \left[\frac{H - H^{**}}{H}\right]\frac{dH}{dt} + \left[\frac{R - R^{**}}{R}\right]\frac{dR}{dt}.\end{aligned}$$

By replacing the values of the time derivatives of state variables of the model (Eq. (2)), we get

$$\begin{aligned}\frac{d\mathscr{L}}{dt} = &\left[\frac{S - S^{**}}{S}\right]\Big[\Pi - (\alpha_1I_I + \alpha_2I_C + \alpha_3I_{IC})S - \mu S\Big]\\ &+ \left[\frac{E - E^{**}}{E}\right]\Big[(\alpha_1I_I + \alpha_2I_C + \alpha_3I_{IC})S - (\beta_1 + \beta_2 + \beta_3 + \mu)E\Big]\\ &+ \left[\frac{I_I - I_I^{**}}{I_I}\right]\Big[\beta_1E - (\gamma_1 + \gamma_2 + \gamma_3 + \mu + d_1)I_I\Big] + \left[\frac{I_C - I_C^{**}}{I_C}\right]\Big[\beta_2E - (\tau_1 + \tau_2 + \tau_c + \mu + d_2)I_C\Big]\\ &+ \left[\frac{I_{IC} - I_{IC}^{**}}{I_{IC}}\right]\Big[\beta_3E + \gamma_1I_I + \tau_1I_C - (\delta_1 + \delta_2 + \mu + d_3)I_{IC}\Big]\\ &+ \left[\frac{H - H^{**}}{H}\right]\Big[\phi_1T - (\phi_3 + \mu + d_5)H\Big]\\ &+ \left[\frac{T - T^{**}}{T}\right]\Big[\gamma_2I_I + \tau_2I_C + \delta_1I_{IC} - (\phi_1 + \phi_2 + \mu + d_4)T\Big]\\ &+ \left[\frac{R - R^{**}}{R}\right]\Big[\gamma_3I_I + \tau_cI_C + \delta_2I_{IC} + \phi_2T + \phi_3H - \mu R\Big].\end{aligned}$$

$$\frac{d\mathscr{L}}{dt} = \xi_1 - \xi_2,$$

where

$$\begin{aligned}
\xi_1 = {} & \Pi + (\alpha_1 I_I + \alpha_2 I_C + \alpha_3 I_{IC} + \mu)\frac{(S^{**})^2}{S} + (\alpha_1 I_I + \alpha_2 I_C + \alpha_3 I_{IC})S + (\beta_1 + \beta_2 + \beta_3 + \mu)\frac{(E^{**})^2}{E} + \beta_1 E \\
& + (\gamma_1 + \gamma_2 + \gamma_3 + \mu + d_1)\frac{(I_I^{**})^2}{I_I} + \beta_2 E + (\tau_1 + \tau_2 + \tau_c + \mu + d_2)\frac{(I_C^{**})^2}{I_C} + \beta_3 E + \gamma_1 I_I + \tau_1 I_C \\
& + (\delta_1 + \delta_2 + \mu + d_3)\frac{(I_{IC}^{**})^2}{I_{IC}} + \gamma_2 I_I + \tau_2 I_C + \delta_1 I_{IC} + (\phi_1 + \phi_2 + \mu + d_4)\frac{(T^{**})^2}{T} + \phi_1 T \\
& + (\phi_3 + \mu + d_5)\frac{(H^{**})^2}{H} + \gamma_3 I_I + \tau_c I_C + \delta_2 I_{IC} + \phi_2 T + \phi_3 H + \mu\frac{(R^{**})^2}{R},
\end{aligned}$$

and

$$\begin{aligned}
\xi_2 = {} & (\alpha_1 I_I + \alpha_2 I_C + \alpha_3 I_{IC} + \mu)\frac{(S - S^{**})^2}{S} + \Pi\frac{S^{**}}{S} + (\alpha_1 I_I + \alpha_2 I_C + \alpha_3 I_{IC} + \mu)S^{**} \\
& + \frac{(E - E^{**})^2}{E}(\beta_1 + \beta_2 + \beta_3 + \mu) + \frac{E^{**}}{E}(\alpha_1 I_I + \alpha_2 I_C + \alpha_3 I_{IC}) + (\beta_1 + \beta_2 + \beta_3 + \mu)E^{**} \\
& + \frac{(I_I - I_I^{**})^2}{I_I}(\gamma_1 + \gamma_2 + \gamma_3 + \mu + d_1) + \frac{I_I^{**}}{I_I}\beta_1 E + (\gamma_1 + \gamma_2 + \gamma_3 + \mu + d_1)I_I^{**} \\
& + \frac{(I_C - I_C^{**})^2}{I_C}(\tau_1 + \tau_2 + \tau_c + \mu + d_2) + \frac{I_C^{**}}{I_C}\beta_2 E + (\tau_1 + \tau_2 + \tau_c + \mu + d_2)I_C^{**} \\
& + \frac{(I_{IC} - I_{IC}^{**})^2}{I_{IC}}(\delta_1 + \delta_2 + \mu + d_3) + \frac{I_{IC}^{**}}{I_{IC}}(\beta_3 E + \gamma_1 I_I + \tau_1 I_C) + (\delta_1 + \delta_2 + \mu + d_3)I_{IC}^{**} \\
& + \frac{(T - T^{**})^2}{T}(\phi_1 + \phi_2 + \mu + d_4) + \frac{T^{**}}{T}(\gamma_2 I_I + \tau_2 I_C + \delta_1 I_{IC}) + (\phi_1 + \phi_2 + \mu + d_4)T^{**} \\
& + \frac{(H - H^{**})^2}{H}(\phi_3 + \mu + d_5) + \frac{H^{**}}{H}(\phi_1) + (\phi_3 + \mu + d_5)H^{**} + \mu\frac{(R - R^{**})^2}{R} + \mu R^{**} \\
& + \frac{R^{**}}{R}(\gamma_3 I_I + \tau_c I_C + \delta_2 I_{IC} + \phi_2 T + \phi_3 H).
\end{aligned}$$

For $\mathscr{R}_0 < 1$, we know $N = S$, and $E = I_I = I_C = I_{IC} = T = H = R = 0$. Therefore, for $\mathscr{R}_0 > 1$, all the state functions are increasing functions except S (which is decreasing) and bounded by endemic equilibrium point P^{**}. Now it is clear that $\xi_2 > \xi_1$ and $\frac{d\mathscr{L}}{dt} < 0$ except at endemic equilibrium (EE) point.

Now, if we put EE point, $S = S^{**}$, $E = E^{**}$, $I_I = {I_I}^{**}$, $I_C = {I_C}^{**}$, $I_{IC} = {I_{IC}}^{**}$, $T = T^{**}$, $H = H^{**}$, and $R = R^{**}$, then

$$\xi_1 = \Pi + (\alpha_1 I_I^{**} + \alpha_2 I_C^{**} + \alpha_3 I_{IC}^{**} + \mu)(S^{**}) + (\alpha_1 I_I^{**} + \alpha_2 I_C^{**} + \alpha_3 I_{IC}^{**})S^{**} + (\beta_1 + \beta_2 + \beta_3 + \mu)(E^{**}) + \beta_1 E^{**} + (\gamma_1 + \gamma_2 + \gamma_3 + \mu + d_1)(I_I^{**}) + \beta_2 E^{**} + (\tau_1 + \tau_2 + \tau_c + \mu + d_2)(I_C^{**}) + \beta_3 E^{**} + \gamma_1 I_I^{**} + \tau_1 I_C^{**} + (\delta_1 + \delta_2 + \mu + d_3)(I_{IC}^{**}) + \gamma_2 I_I^{**} + \tau_2 I_C^{**} + \delta_1 I_{IC}^{**} + (\phi_1 + \phi_2 + \mu + d_4)(T^{**}) + \phi_1 T^{**} + (\phi_3 + \mu + d_5)(H^{**}) + \gamma_3 I_I^{**} + \tau_c I_C^{**} + \delta_2 I_{IC}^{**} + \phi_2 T^{**} + \phi_3 H^{**} + \mu(R^{**}),$$

and

$$\xi_2 = \Pi + (\alpha_1 I_I^{**} + \alpha_2 I_C^{**} + \alpha_3 I_{IC}^{**} + \mu)S^{**} + (\alpha_1 I_I^{**} + \alpha_2 I_C^{**} + \alpha_3 I_{IC}^{**})S^{**} + (\beta_1 + \beta_2 + \beta_3 + \mu)E^{**} + \beta_1 E^{**} + (\gamma_1 + \gamma_2 + \gamma_3 + \mu + d_1)I_I^{**} + \beta_2 E^{**} + (\tau_1 + \tau_2 + \tau_c + \mu + d_2)I_C^{**} + \beta_3 E^{**} + \gamma_1 I_I^{**} + \tau_1 I_C^{**} + (\delta_1 + \delta_2 + \mu + d_3)I_{IC}^{**} + (\gamma_2 I_I^{**} + \tau_2 I_C^{**} + \delta_1 I_{IC}^{**}) + (\phi_1 + \phi_2 + \mu + d_4)T^{**} + \phi_1 T^{**} + (\phi_3 + \mu + d_5)H^{**} + \gamma_3 I_I^{**} + \tau_c I_C^{**} + \delta_2 I_{IC}^{**} + \phi_2 T^{**} + \phi_3 H^{**} + uR^{*} * .$$

Thus, $\frac{d\mathscr{L}}{dt} = 0$ at EE point P^{**}, implies that

$$\frac{d\mathscr{L}}{dt} \leq 0. \tag{24}$$

Thus, LaSalle's invariance principle [28] guarantee that the endemic equilibrium (EE) point P^{**} is globally asymptotically stable (GAS). ■

5 Sensitivity Analysis

Sensitivity analysis is needed to design efficient viral control strategies. Our goal is to find parameters that are extremely sensitive to $\mathscr{R}_0$. Targeting parameters with a high sensitivity index can help manage epidemics since they are thought to be extremely sensitive to $\mathscr{R}_0$. We apply the method described in [29] and applied in [28,30,32] to determine the sensitivity index of a parameter p using the formula:

$$\bigcap_p^{\mathscr{R}_0} = \frac{\partial \mathscr{R}_0}{\partial p}\frac{p}{\mathscr{R}_0}. \tag{25}$$

We calculate the sensitivity indices for every parameter used in $\mathscr{R}_0$ (Table 1). The force of infection of corona α_2 and the force of infection of influenza α_1 are the nontrivial most sensitive parameters to $\mathscr{R}_0$ according to the sensitivity analysis. Π and μ are the trivial most sensitive parameters. It is also notable that treatment rates of infections are not very sensitive. Sensitivity analysis is an effective technique for determining the factors that matter most in limiting the spread of infections. To visualize how each parameter affects each of $\mathscr{R}_I$, $\mathscr{R}_C$, $\mathscr{R}_{IC}$, and $\mathscr{R}_0$, respectively, we plot all of them against each parameter (Figs. 5–7).

Table 1: Sensitivity Index for reproduction number $\mathscr{R}_0$ for all model parameters. The force parameter α_1 (influenza) and α_2 (corona) are the most sensitive. The parameters that have a sensitivity index of zero indicate that they have no effect on $\mathscr{R}_0$

Parameter	Values	Sensitivity index	Reference
μ	0.25	−1.599206014	[9]
Π	2.5	0.9999	[9]
α_1	0.203	0.4175689517	[22]

(Continued)

Table 1 (continued)

Parameter	Values	Sensitivity index	Reference
α_2	0.5249	0.5207162090	[22]
α_3	0.0203	0.06171483879	Assume
β_1	0.4	0.1201630446	[22]
β_2	0.235	0.3378368317	[9]
β_3	0.4	−0.2634473476	[22]
γ_1	0.002	−0.001291547766	[22]
γ_2	0.1	−0.07292876733	Assume
γ_3	0.1998	−0.1457116771	[22]
τ_1	0.2	−0.1394682056	Assume
τ_2	0.1	−0.07658965883	Assume
τ_c	0.13978	−0.1070570251	[22]
δ_1	0.1	−0.01234296782	Assume
δ_2	0.125	−0.01542870978	[22]
d_1	0.021	−0.01531504114	[22]
d_2	0.008	−0.06127172706	[22]
d_3	0.025	−0.003085741955	[22]
ϕ_1	0.02	0	Assume
ϕ_2	0.8	0	Assume
ϕ_3	0.125	0	[19]
d_4	0.02	0	Assume
d_5	0.02	0	Assume

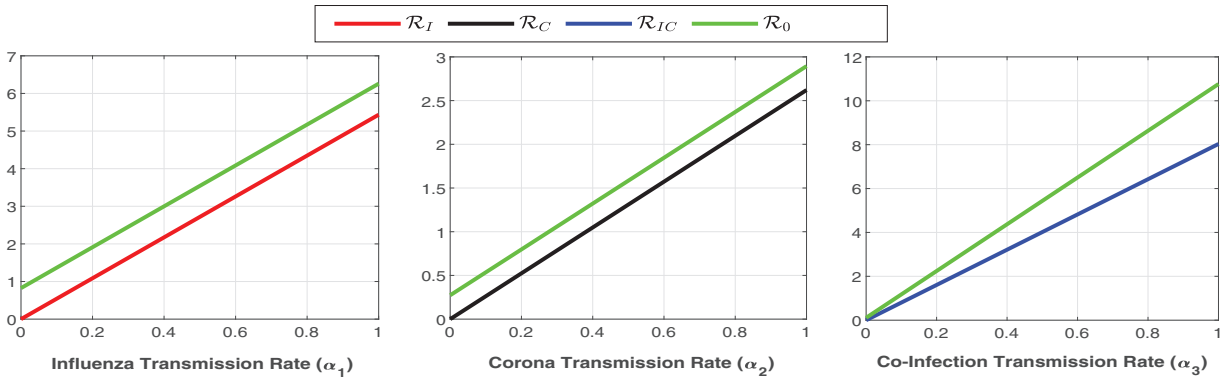

Figure 5: (Continued)

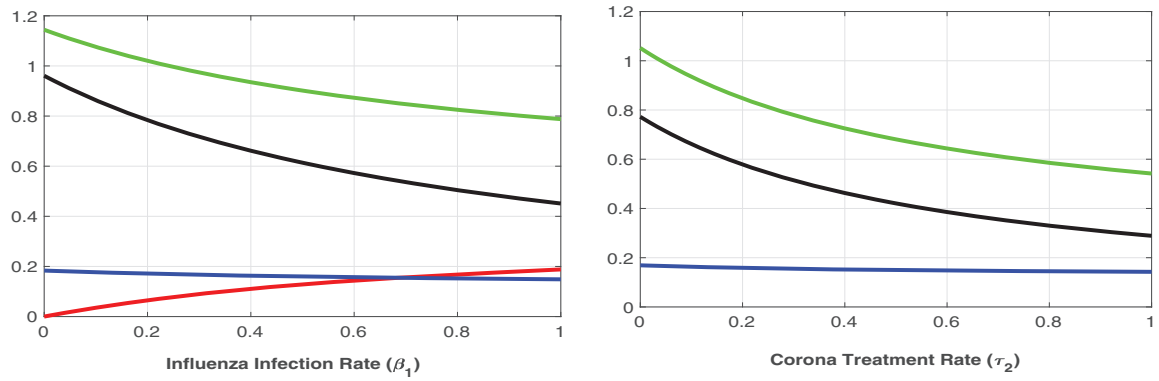

Figure 5: Plot of $\mathscr{R}_I$, $\mathscr{R}_C$, $\mathscr{R}_{IC}$, and $\mathscr{R}_0$ reproduction numbers against select model parameters for transmission rates $(\alpha_1, \alpha_2, \alpha_3)$ and translation rate of influenza (β_1 and τ_2). Here, red, black, blue, and green represent the $\mathscr{R}_I$, $\mathscr{R}_C$, $\mathscr{R}_{IC}$, and $\mathscr{R}_0$, respectively. The increasing and decreasing curves of the reproduction numbers represent the effect of those parameters on the reproduction numbers. The missing curves show that the corresponding reproduction number is independent of that parameter

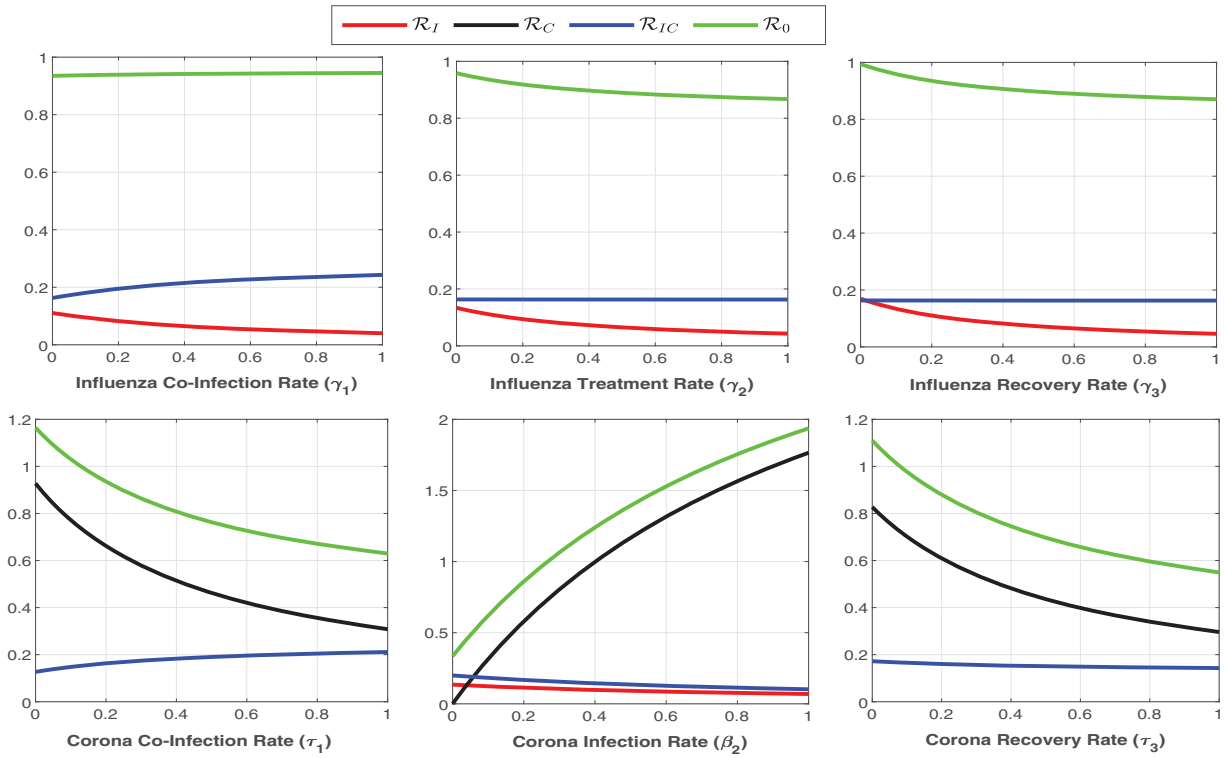

Figure 6: Plot of $\mathscr{R}_I$, $\mathscr{R}_C$, $\mathscr{R}_{IC}$, and $\mathscr{R}_0$ reproduction numbers *vs.* parameters for flu translation rate (γ_1), flu treatment (γ_2), and recovery rate (γ_3), etc. Since the green curve is the sum of the reproduction numbers of all the submodels, it is therefore always dominant in all cases

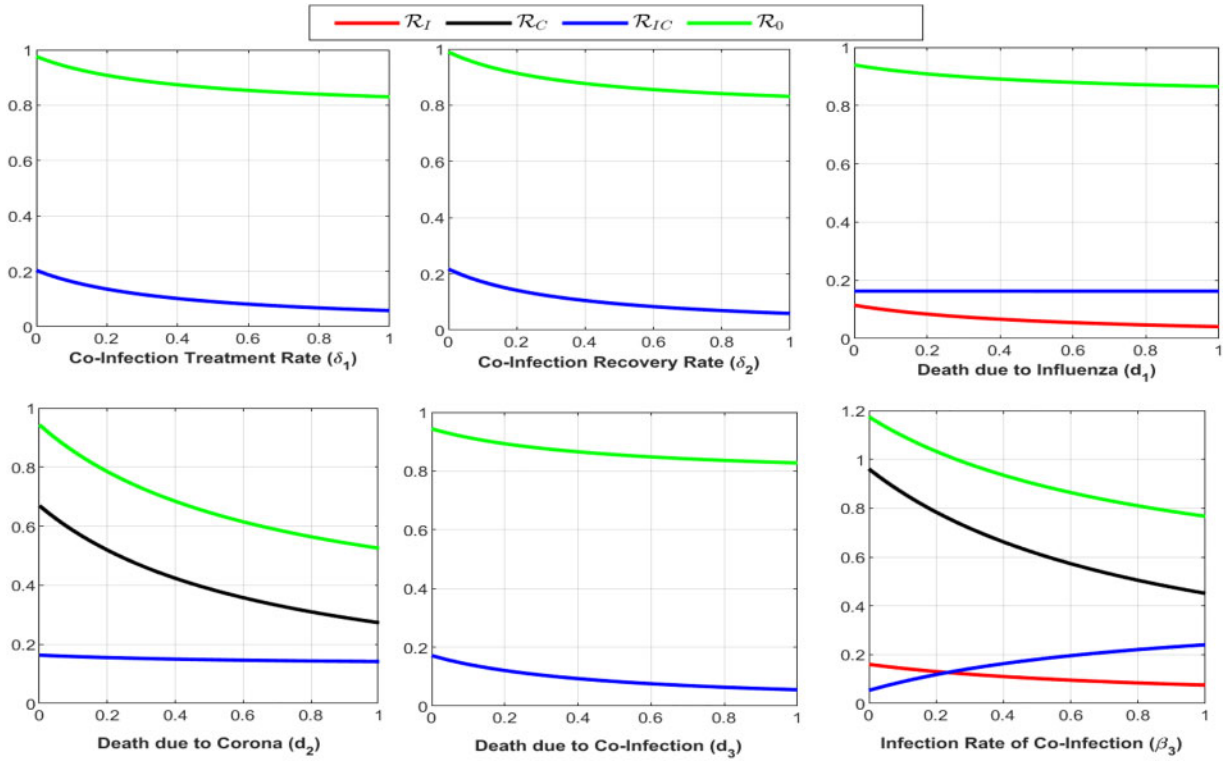

Figure 7: Plot of reproduction numbers $\mathscr{R}$'s *vs*. model parameters with negative sensitivity index

6 Control Analysis

In this section, we will provide a comprehensive analysis of different control analysis. We will perform both the fixed control and optimal control analysis with different control parameters [33–37].

6.1 Updated Model

To provide insightful information and realistic analysis, we update the proposed model (Eq. (2)) with a new non-pharmaceutical parameter s, and named as self-precaution taken by susceptible populations. Thus, the updated model can be written as:

$$\frac{dS}{dt} = \Pi - (\alpha_1 I_I + \alpha_2 I_C + \alpha_3 I_{IC})S - (\mu + s)S, \tag{26a}$$

$$\frac{dE}{dt} = (\alpha_1 I_I + \alpha_2 I_C + \alpha_3 I_{IC})S - (\beta_1 + \beta_2 + \beta_3 + \mu)E, \tag{26b}$$

$$\frac{dI_I}{dt} = \beta_1 E - (\gamma_1 + \gamma_2 + \gamma_3 + \mu + d_1)I_I, \tag{26c}$$

$$\frac{dI_C}{dt} = \beta_2 E - (\tau_1 + \tau_2 + \tau_c + \mu + d_2)I_C, \tag{26d}$$

$$\frac{dI_{IC}}{dt} = \beta_3 E + \gamma_1 I_I + \tau_1 I_C - (\delta_1 + \delta_2 + \mu + d_3) I_{IC}, \tag{26e}$$

$$\frac{dT}{dt} = \gamma_2 I_I + \tau_2 I_C + \delta_1 I_{IC} - (\phi_1 + \phi_2 + \mu + d_4) T, \tag{26f}$$

$$\frac{dH}{dt} = \phi_1 T - (\phi_3 + \mu + d_5) H, \tag{26g}$$

$$\frac{dR}{dt} = sS + \gamma_3 I_I + \tau_c I_C + \delta_2 I_{IC} + \phi_2 T + \phi_3 H - \mu R, \tag{26h}$$

with the non-negative initial conditions

$$S(0) > 0, \quad E(0) \geq 0, \quad I_I(0) \geq 0, \quad I_C(0) \geq 0, \; I_{IC}(0) \geq 0, \quad H(0) \geq 0, \quad T(0) \geq 0, \quad R(0) \geq 0. \tag{26i}$$

6.2 Effect of Different Control Levels

Here we investigate the influence of self-precaution and treatment rates on the dynamics of state variables in the updated model (Eq. (26)), with a particular focus on those representing infection within the population. Employing various precautions and treatment levels spanning from 0% to 80%, we examine their effects on disease control. The findings indicate a decline in the number of infectious cases as the treatment level increases. Consequently, we can deduce that an elevated treatment rate for infectious classes correlates with a reduction in infection. It is clear from Figs. 8–10, treatment can reduce infection, but it cannot permanently eradicate the co-infection disease. On the other hand, self-precaution, (e.g., social distancing, the wearing of a mask, and the regular use of handwash) is an efficient non-pharmaceutical way to protect oneself and to help to eradicate the disease from the population (Fig. 11). Based on analysis of different aspects of the disease dynamics and cost of controls, self-precaution is the best policy to eradicate the disease. The combined effect of all treatment parameters with and without self-precautions will be presented in the next section.

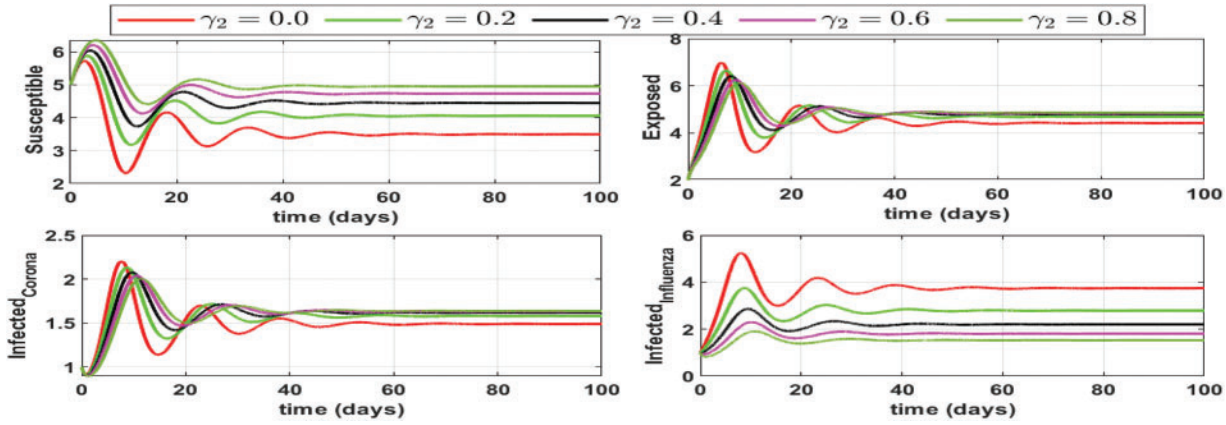

Figure 8: (Continued)

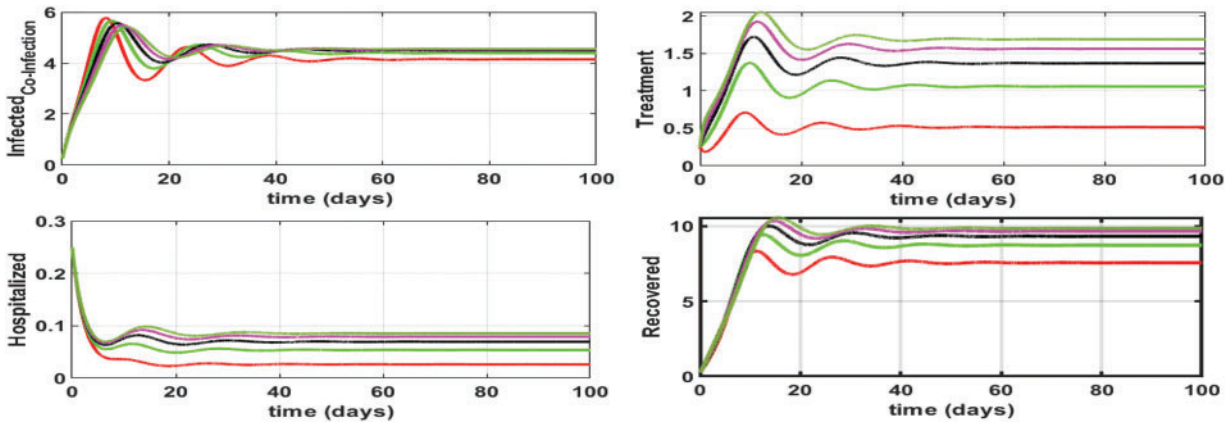

Figure 8: Impact of influenza treatment rate (γ_2) on influenza and corona dynamics (model Eq. (26)). Disease is at its peak at $\gamma_2 = 0$ and decreases with the increase in treatment, ($\gamma_2 = 0.2, \gamma_2 = 0.4, \gamma_2 = 0.6,$ and $\gamma_2 = 0.8$). We assume that we have treatment resources up to 80%, and it has minimized almost all the infectious compartment but has a maximum impact on the dynamics of influenza infectious

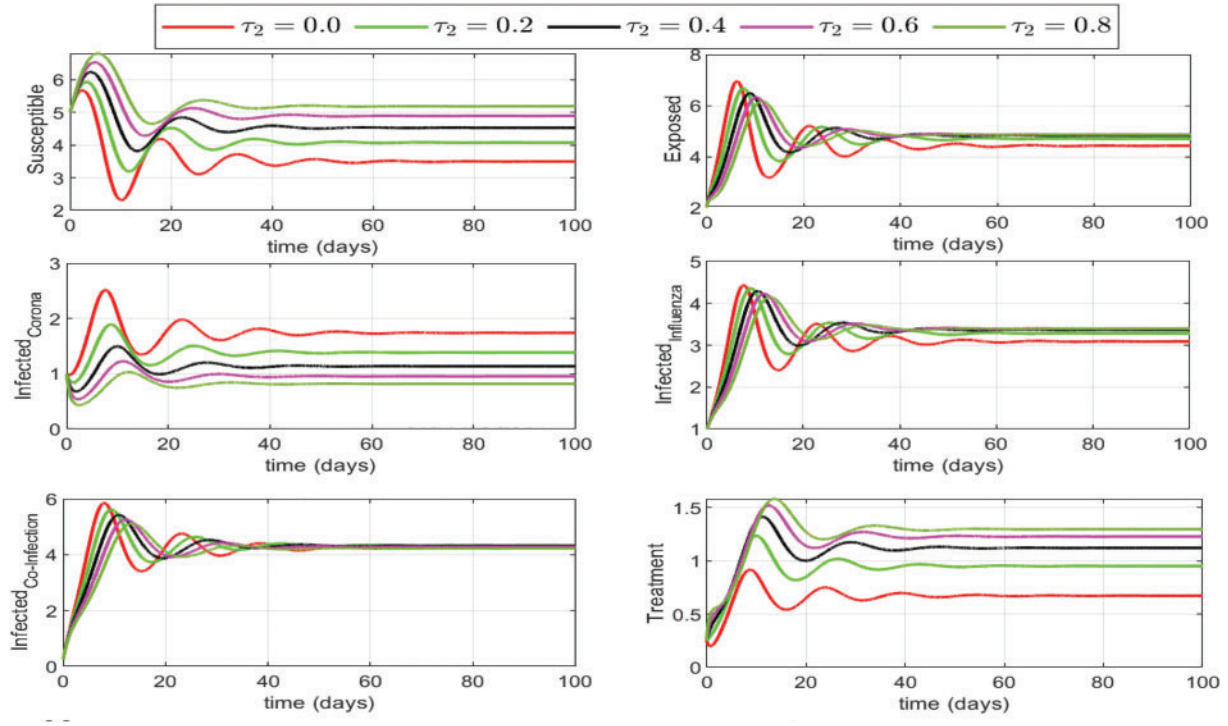

Figure 9: (Continued)

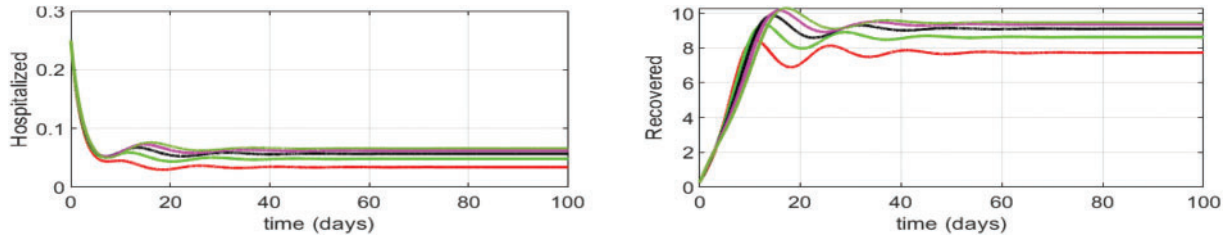

Figure 9: Different levels of treatment rate τ_2 (model Eq. (26)) for the patients infected with coronavirus only and it is assumed that treatment parameter τ_2 attains 0% to 80% with an increment of 20%. The dynamics decrease with the increase of treatment rate and vice versa. The infectious with corona are decreasing to their minimum level with a maximum treatment rate

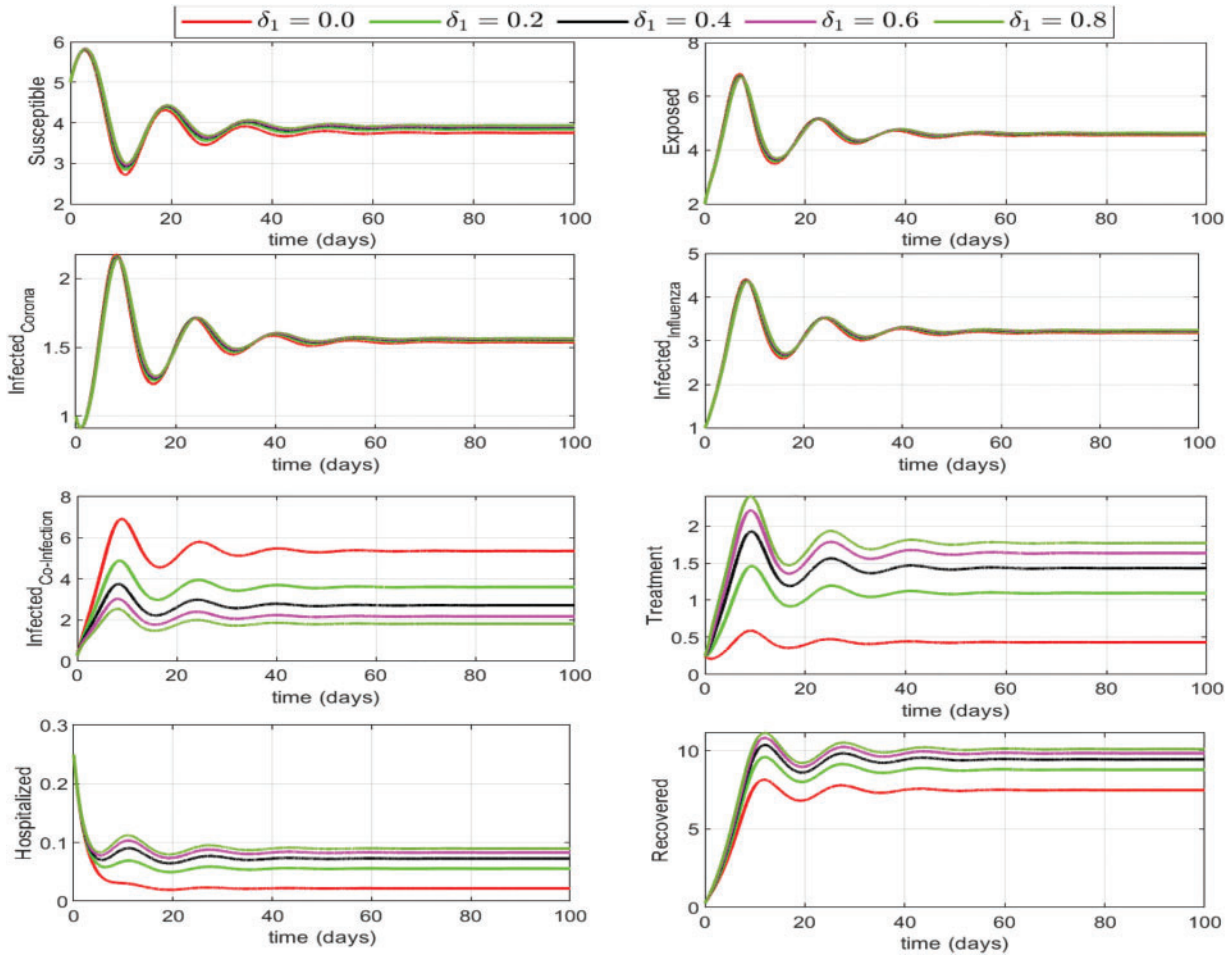

Figure 10: Effect of influenza-corona co-infection treatment rate δ_1 on model dynamics (Eq. (26)). Interestingly, there is almost no impact on the dynamics of susceptible, exposed, influenza infectious, and corona infectious. However, treatment and recovery increased

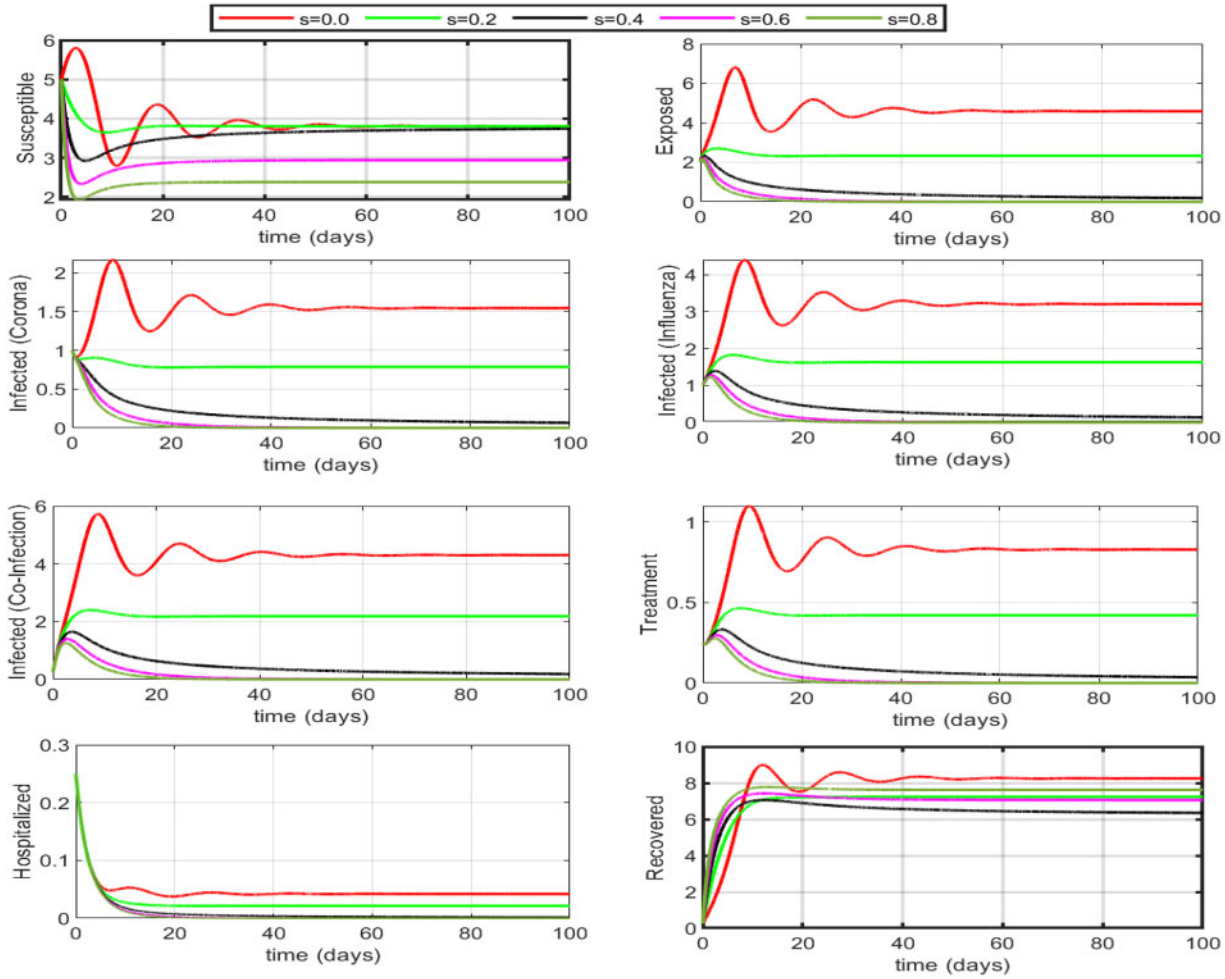

Figure 11: Impact of self-precaution on the dynamics assuming that if someone is taking precautions, they are recovered by default. If 50% to 60% (self-precaution s = 0.5 or 0.6) of the susceptible population is aware of the disease and is taking safety measures (i.e., social distancing, hand washing, etc.), then the disease will die out within a few days. Self-precaution not only helps eradicate the disease but also decreases the number of under-treatments individuals and the burden on hospitalized

6.3 Optimal Control Analysis

In this section, we will define an optimal control problem to find the optimal treatment rates and self-precaution measures as time-dependent controls. We perform optimal control analysis for model (Eq. (26))using the Pontryagin maximum principle (PMP). The objective functional to be minimized is defined as follows:

$$J(E, I_I, I_C, I_{IC}, u_1, u_2, u_3, u_4) = \int_0^{\mathbb{T}} A_1 E(t) + A_2 I_I(t) + A_3 I_C + A_4 I_{IC} + B_1 \frac{u_1^2(t)}{2} + B_2 \frac{u_2^2(t)}{2} + B_3 \frac{u_3^2(t)}{2} + B_4 \frac{u_4^2(t)}{2} dt, \tag{27}$$

where $\mathbb{T}$ represents the final time. $E(t), I_I(t), I_C(t), I_{IC}(t)$ are the infectious state variables, and $u_1(t), u_2(t), u_3(t)$ and $u_4(t)$ are our control variables for treatment of infectious compartments (i.e., γ_2, τ_2, and δ_1), and self-precaution measures s taken by susceptible, respectively. B_1, B_2, B_3, and B_4 are the associated cost parameters with our respective time-dependent controls.

The object is to find the optimal control $u^*(t) = (u_1, u_2, u_3, u_4) \in U$ so that objective functional Eq. (27) is minimized.

6.3.1 Necessary Optimality Conditions

For PMP optimization, we construct the following Hamiltonian

$$H(t, y, u_1, u, \lambda_j) = A_1E + A_2I_I + A_3I_C + A_4I_{IC} + B_1\frac{u_1^2(t)}{2} + B_2\frac{u_2^2(t)}{2} + B_3\frac{u_3^2(t)}{2} + B_4\frac{u_4^2(t)}{2} + \sum_{j=1}^{8} L_j f_j(t, y, u).$$

We denote the state variables by $y = (S, E, I_I, I_C, I_{IC}, T, H, R)$. The adjoint variables and the right-hand side of our system of state equations are denoted by L_j and $f_j(t, y, u)$, respectively, where $j = 1, 2, 3, \ldots, 8$.

$$\begin{aligned} H(t, y, u, L_i) = {} & A_1E + A_2I_I + A_3I_C + A_4I_{IC} + B_1\frac{u_1^2(t)}{2} + B_2\frac{u_2^2(t)}{2} + B_3\frac{u_3^2(t)}{2} + B_4\frac{u_4^2(t)}{2} \\ & + L_1(\Pi - (\alpha_1I_I + \alpha_2I_C + \alpha_3I_{IC})S - (\mu + u_4)S) + L_2(\alpha_1I_I + \alpha_2I_C + \alpha_3I_{IC})S \\ & - L_2(\beta_1 + \beta_2 + \beta_3 + \mu)E + L_3(\beta_1E - (\gamma_1 + u_1 + \gamma_3 + \mu + d_1)I_I) \\ & + L_4(\beta_2E - (\tau_1 + u_2 + \tau_c + \mu + d_2)I_C) + L_5(\beta_3E + \gamma_1I_I + \tau_1I_C - (u_3 + \delta_2 + \mu + d_3)I_{IC}) \\ & + L_6(u_1I_I + u_2I_C + u_3I_{IC} - (\phi_1 + \phi_2 + \mu + d_4)T) + L_7(\phi_1T - (\phi_3 + \mu + d_5)H) \\ & + L_8(u_4S + \gamma_3I_I + \tau_cI_C + \delta_2I_{IC} + \phi_2T + \phi_3H - \mu R). \end{aligned} \tag{28}$$

The First condition of optimality is given by

$$\frac{\partial H}{\partial u} = 0.$$

The PMP gives us the following expressions for the controls

$$\frac{\partial H}{\partial u_1} = 0 \Longrightarrow u_1(t) = \frac{I_I(L_3 - L_6)}{B_1}, \tag{29a}$$

$$\frac{\partial H}{\partial u_2} = 0 \Longrightarrow u_2(t) = \frac{I_C(L_4 - L_6)}{B_2}, \tag{29b}$$

$$\frac{\partial H}{\partial u_3} = 0 \Longrightarrow u_3(t) = \frac{I_{IC}(L_5 - L_6)}{B_3}, \tag{29c}$$

$$\frac{\partial H}{\partial u_4} = 0 \Longrightarrow u_4(t) = \frac{S(L_1 - L_8)}{B_4}. \tag{29d}$$

Under the max-min bounds, we update the controls to have

$$u_1^*(t) = min\left[u_{1(max)}, max\left(0, \frac{I_I(L_3 - L_6)}{B_1}\right)\right], \tag{30a}$$

$$u_2^*(t) = min\left[u_{2(max)}, max\left(0, \frac{I_C(L_4 - L_6)}{B_2}\right)\right], \tag{30b}$$

$$u_3^*(t) = min\left[u_{3(max)}, max\left(0, \frac{I_{IC}(L_5 - L_6)}{B_3}\right)\right], \tag{30c}$$

$$u_4^*(t) = min\left[u_{2(max)}, max\left(0, \frac{S(L_1 - L_8)}{B_4}\right)\right]. \tag{30d}$$

Using the second optimality condition

$$\frac{dL_j}{dt} = -\frac{\partial H}{\partial y_j}, \quad j = 1, 2, 3, \ldots, 8, \tag{31}$$

We get the following adjoint equations

$$\frac{dL_1}{dt} = (\alpha_1 I_I + \alpha_2 I_C + \alpha_3 * I_{IC} + \mu)L_1 + u_4 L_1 - (\alpha_1 I_I + \alpha_2 I_C + \alpha_3 I_{IC})L_2 - u_4 L_8, \tag{32a}$$

$$\frac{dL_2}{dt} = (\beta_1 + \beta_2 + \beta_3 + \mu)L_2 - \beta_1 L_3 - \beta_2 L_4 - \beta_3 L_5 - A_1, \tag{32b}$$

$$\frac{dL_3}{dt} = \alpha_1 S(L_1 - l_2) + (\gamma_1 + u_1 + \gamma_3 + \mu + d_1)L_3 - \gamma_1 L_5 - u_1 L_6 - \gamma_3 L_8 - A_2, \tag{32c}$$

$$\frac{dL_4}{dt} = \alpha_2 S(L_1 - L_2) + (\tau_1 + u_2 + \tau_c + \mu + d_2)L_4 - \tau_1 L_5 - u_2 L_6 - \tau_c L_8 - A_3, \tag{32d}$$

$$\frac{dL_5}{dt} = \alpha_3 S(L_1 - L_2) + (u_3 + \delta_2 + \mu + d_3)L_5 - u_3 L_6 - \delta_2 L_8 - A_4, \tag{32e}$$

$$\frac{dL_6}{dt} = (\phi_1 + \phi_2 + \mu + d_4)L_6 - \phi_1 L_7 - \phi_2 L_8, \tag{32f}$$

$$\frac{dL_7}{dt} = (\phi_3 + \mu + d_5)L_7 - \phi_3 L_8, \tag{32g}$$

$$\frac{dL_8}{dt} = \mu L_8, \tag{32h}$$

with $L_i(T_f) = 0,\ i = 1, 2, \ldots, 8.$

6.3.2 Optimal Solution

In the first case, we take all three treatment controls ($u_1 = \gamma_2, u_2 = \tau_2$, and $u_3 = \delta_1$) and ignore the self-precaution control ($u_4 = s = 0$) (Figs. 12 and 13), and in the second case, we observe the combined

effect of the treatment (pharmaceutical) controls and the self-precaution (non-pharmaceutical) control (Figs. 14 and 15). Both control strategies minimize the disease and we attain the minimum value of the corresponding objective functional. The objective functional and treatment rates both are minimum when people are taking self-precaution and the disease dies out in this case in a very short time (Fig. 15). On the other hand, when we only consider treatment controls, disease is reduced but not eliminated (Fig. 13). Thus, treatment can reduce the impact of disease but cannot completely stop its spread without taking precautionary measures.

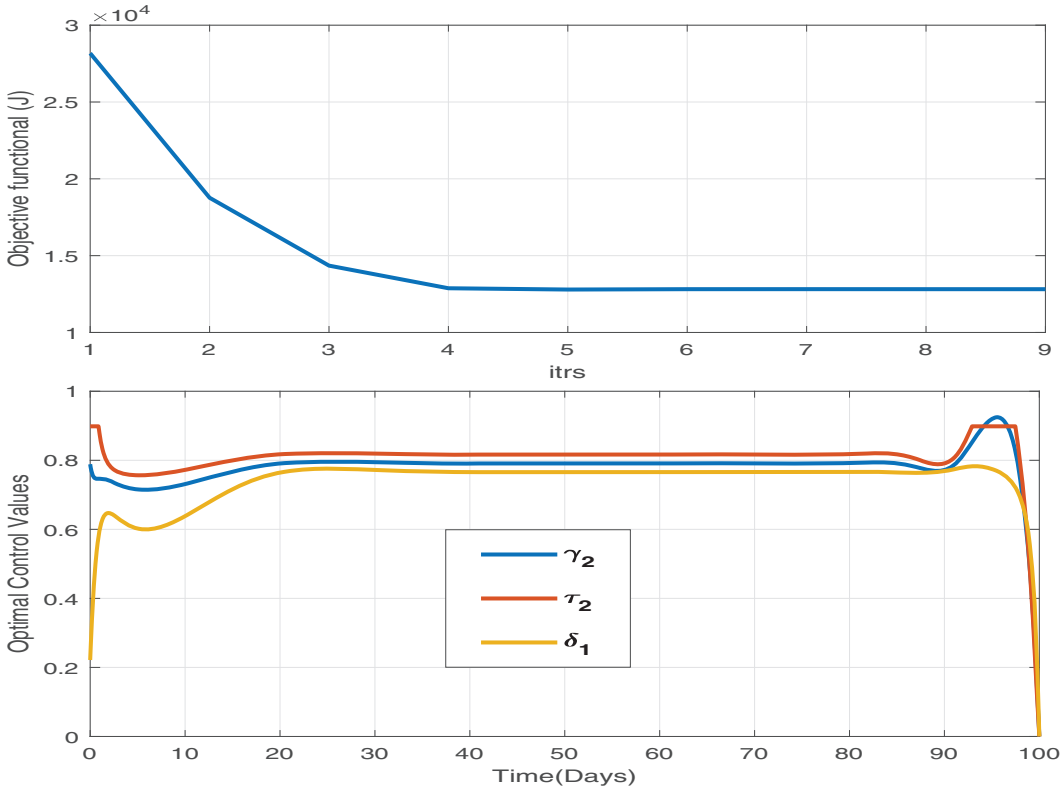

Figure 12: The objective functional and the corresponding optimal control values for parameters γ_2, τ_2 and δ_1 are shown for the first optimal control strategy, where we combine all treatment rates as optimal controls. We assume that our capacity to give treatment is up to 90% and allow controls to get a maximum value of 0.9. All the controls are initially at maximum and then slowly decrease

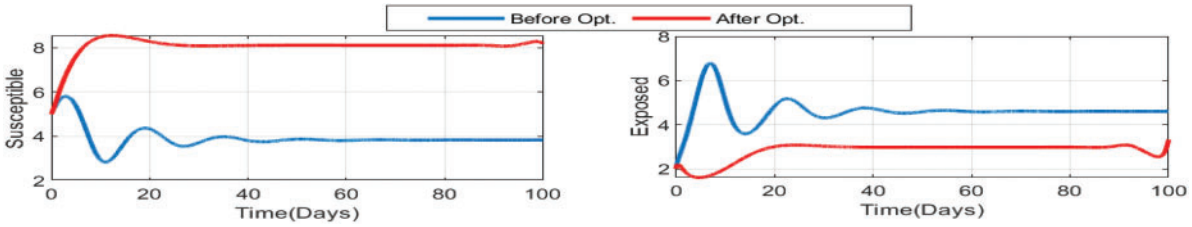

Figure 13: (Continued)

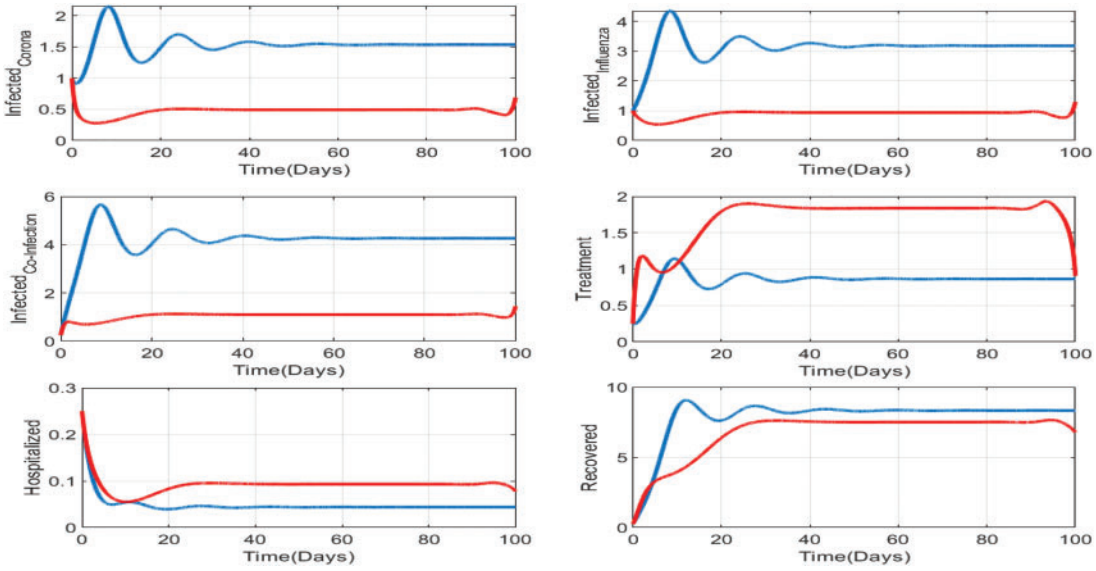

Figure 13: Impact of treatments on the susceptible, exposed, influenza-infective, and corona-infective populations. The red line represents the dynamics of each state variable before the use of optimal treatment controls, and the red line represents the dynamics after applying the optimal controls for 100 days

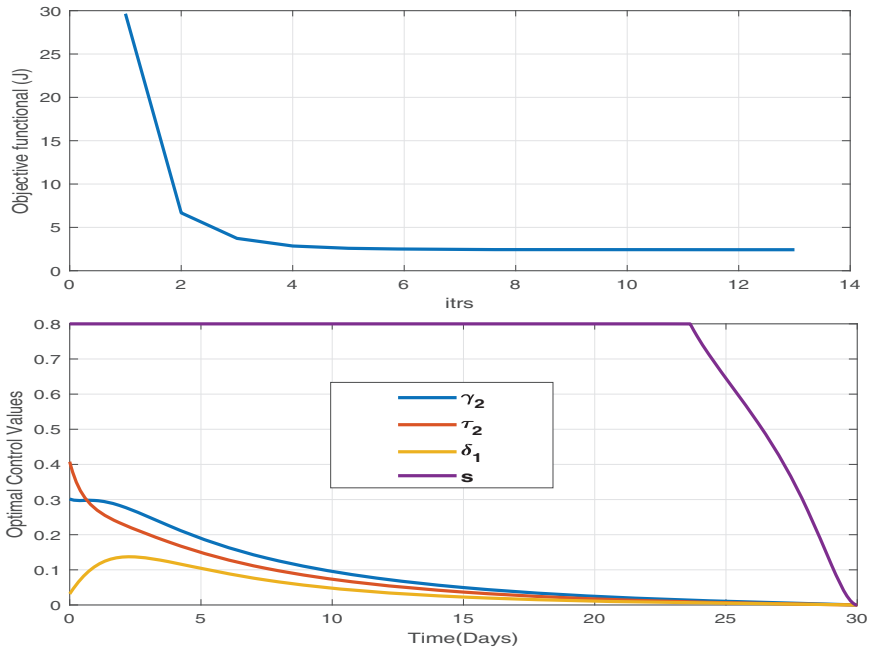

Figure 14: We adopt both pharmaceutical (treatment) and non-pharmaceutical (self-precaution) optimal controls and analyze the effect of this control strategy. This is the best control strategy. It minimizes the burden of disease as well as the cost of treatment. We obtain the minimum value of the objective functional in only 13 iterations, and the maximum level of treatments is 40% and for a very short time

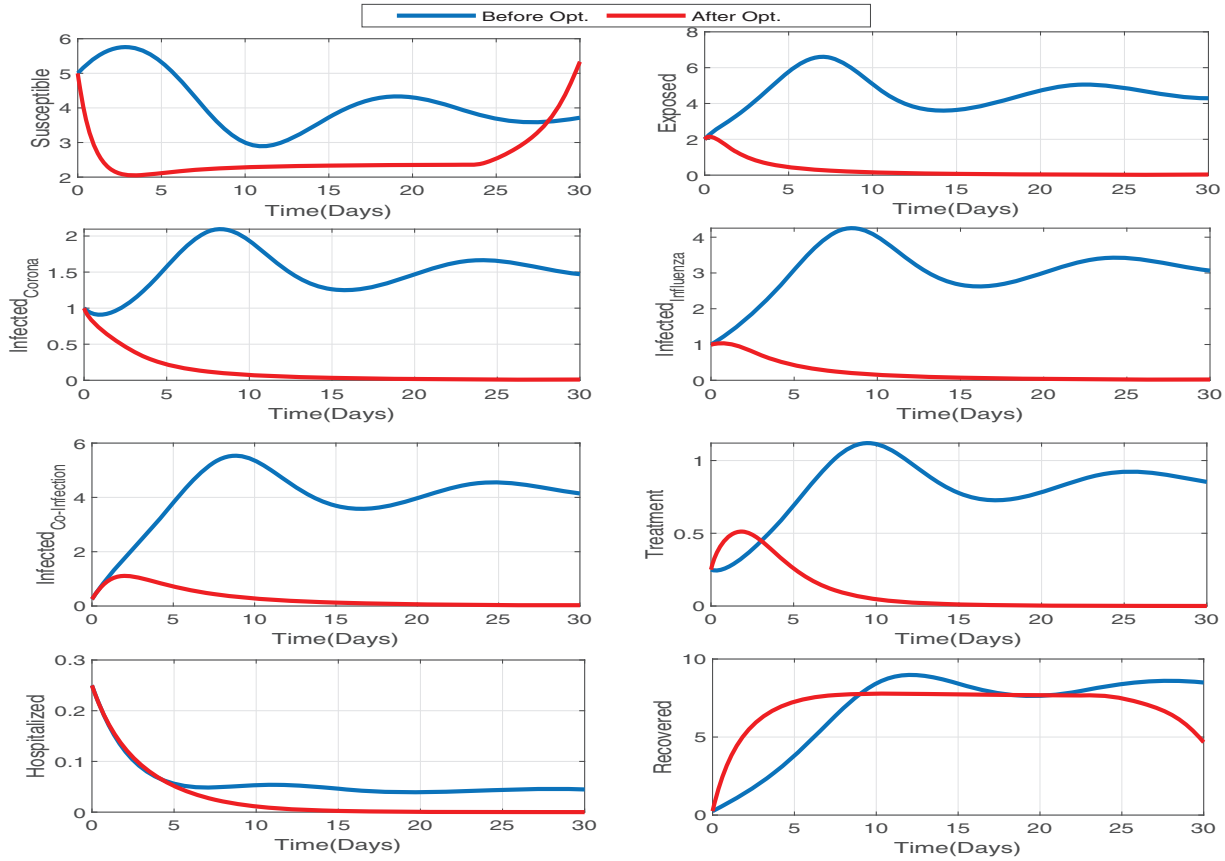

Figure 15: The impact of optimal treatments and self-precaution control has a great impact on the susceptible, exposed, influenza infectious, and corona infectious populations. The blue and red lines represent the dynamics without and with optimal controls. Since red lines reach zero in all the infectious compartments in a very short time, this optimal control is very effective

7 Conclusion

In this manuscript, we have proposed a new $SEI_II_CI_{IC}THR$ mathematical model for influenza-corona co-infection and suggested the optimal control strategies. We analyzed the theoretical properties of the mathematical model and proved that the proposed model is well-posed and has a positive and bounded solution within a feasible region. We also determined the equilibrium points of the model and established the local and global stability of the model at these equilibrium points. To find the most sensitive parameters, we did sensitivity analysis and found that the recruitment rate and death rate are trivial sensitive parameters, and transmission parameters and treatment rates are the most not-trivial direct and inverse, respectively, sensitive parameters. After detailed theoretical analysis, we checked the impact of different levels of treatment on the dynamics of the co-infection disease. Our numerical experiments indicate that all the treatment rates are useful to minimize the effect of the disease but are not able to prevent the disease. We defined an optimal control problem and analyzed the effects of both pharmaceutical and non-pharmaceutical optimal controls. Our findings suggest that treatment alone is able to minimize disease spread; however, the use of self-precaution along with treatment is the best control strategy to eliminate the disease from the population at a minimum cost.

In our upcoming research, we will use a fractional model to provide a thorough depiction of the co-infection dynamics of influenza and coronavirus. This model will use Caputo-Fabrizio (CF) and Atangana-Baleanu Caputo (ABC) derivative operators to represent the intricate interactions between the two illnesses. Furthermore, we will incorporate numerous intervention options, such as immunization, into this framework. Our research will go beyond analyzing the success of these interventions, suggesting optimal approaches to vaccination and hospitalization using a fractional-order optimal control problem. This will enable us to identify the most effective strategies for lowering the co-infection burden on the healthcare systems and improving patient health. In addition to the above, the proposed influenza-corona co-infection model offers valuable insights into dynamics and control strategies but has limitations. It simplifies complex biological and socio-behavioral processes, assumes homogeneous population mixing, and overlooks multi-strain infections, resistance, and co-infections with other diseases, affecting real-world applicability.

Acknowledgement: We would like to thank NASA Oklahoma Established Program to Stimulate Competitive Research (EPSCoR) Infrastructure Development, "Machine Learning Ocean World Biosignature Detection from Mass Spec" (PI: Brett McKinney), and Tandy School of Computer Science, University of Tulsa.

Funding Statement: This work was partly supported by NASA Oklahoma Established Program to Stimulate Competitive Research (EPSCoR) Infrastructure Development, "Machine Learning Ocean World Biosignature Detection from Mass Spec" (PI: Brett McKinney), Grant No. 80NSSC24M0109, and Tandy School of Computer Science, University of Tulsa.

Author Contributions: The authors confirm contribution to the paper as follows: **Muhammad Imran:** Conceptualization, Data curation, Formal analysis, Software, Validation, Writing—original draft. **Brett McKinney:** Supervision, Data curation, Formal analysis, Investigation, Project administration, Resources, Writing—review & editing. **Azhar Iqbal Kashif Butt:** Software, Validation, Visualization, Writing—review & editing. All authors reviewed the results and approved the final version of the manuscript.

Availability of Data and Materials: Data sharing not applicable to this article as no datasets were generated or analyzed during the current study.

Ethics Approval: Not applicable.

Conflicts of Interest: The authors declare no conflicts of interest to report regarding the present study.

References

1. World of Health Organization. Novel Coronavirus (2019-nCoV)–SITUATION REPORT-1. 2020. Available from: https://www.who.int/docs/default-source/coronaviruse/situation-reports/20200121-sitrep-1-2019-ncov.pdf. [Accessed 2024].
2. World of Health Organization. WHO Director-General's opening remarks at the media briefing on COVID-19–11 March 2020. Available from: https://www.who.int/director-general/speeches/detail/who-director-general-s-opening-remarks-at-the-media-briefing-on-covid-19—11-march-2020. [Accessed 2023].
3. Hu B, Huang S, Yin L. The cytokine storm and COVID-19. J Med Virol. 2021 Jan;93(1):250–6. doi:10.1002/jmv.26232.

4. Hui DS, Azhar EI, Madani TA, Ntoumi F, Koch R, Dar O, et al. The continuing 2019-nCoV epidemic threat of novel corona viruses to global health: the latest 2019 novel coronavirus outbreak in Wuhan, China. Int J Infect Dis. 2020;91:264–6.
5. Abioye AI, Peter OJ, Addai E, Oguntolu FA, Ayoola TA. Modeling the impact of control strategies on malaria and COVID-19 coinfection: insights and implications for integrated public health interventions. Qual Quant. 2024;58(4):3475–95. doi:10.1007/s11135-023-01813-6.
6. Ojo MM, Peter OJ, Goufo EFD, Nisar KS. A mathematical model for the co-dynamics of COVID-19 and tuberculosis. Math Comput Simul. 2023;207(3):499–520. doi:10.1016/j.matcom.2023.01.014.
7. Kumar Ghosh J, Saha P, Kamrujjaman M, Ghosh U. Transmission dynamics of COVID-19 with saturated treatment: a case study of spain. Braz J Phys. 2023;53(3):54. doi:10.1007/s13538-023-01267-z.
8. Khondaker F, Kamrujjaman M, Shahidul Islam M. Optimal control analysis of COVID-19 transmission model with physical distance and treatment. Adv Biol Res. 2022;3(1):65–76.
9. Butt AIK, Imran M, Batool S, Nuwairan MA. Theoretical analysis of a COVID-19 CF-fractional model to optimally control the spread of pandemic. Symmetry. 2023;15(2):380. doi:10.3390/sym15020380.
10. Mohsen A, AL-Husseiny HF, Zhou X, Hattaf K. Global stability of COVID-19 model involving the quarantine strategy and media coverage effects. AIMS Pub Health. 2020;7(3):587–605.
11. World of Health Organization. COVID-19 epidemiological update–24 November 2023. Available from: https://www.who.int/publications/m/item/covid-19-epidemiological-update-24-november-2023. [Accessed 2023].
12. World of Health Organization. Influenza (Seasonal). 2023 Oct 3. Available from: https://www.who.int/news-room/fact-sheets/detail/influenza-(seasonal). [Accessed 2023].
13. Taubenberger JK, Morens DM. 1918 influenza: the mother of all pandemics. Emerg Infect Dis. 2006 Jan;12(1):15–22. doi:10.3201/eid1201.050979.
14. World of Health Organization. 70 years of GISRS–the global influenza surveillance & response system. Available from: https://www.who.int/news-room/feature-stories/detail/seventy-years-of-gisrs–the-global-influenza-surveillance—response-system. [Accessed 2024].
15. CDC. Key Facts About Influenza (Flu). Available from: https://www.cdc.gov/flu/about/keyfacts. [Accessed 2024].
16. Tang CY, Boftsi M, Staudt L, McElroy JA, Li T, Duong S, et al. SARS-CoV-2 and influenza co-infection: a cross-sectional study in central Missouri during the 2021–2022 influenza season. Virology. 2022 Nov;576(10):105–10. doi:10.1016/j.virol.2022.09.009.
17. Arguni E, Supriyati E, Hakim MS, Daniwijaya EW, Makrufardi F, Rahayu A, et al. Co-infection of SARS-CoV-2 with other viral respiratory pathogens in Yogyakarta, Indonesia: a cross-sectional study. Ann Med Surg. 2022 May;77:103676. doi:10.1016/j.amsu.2022.103676.
18. Peter OJ, Panigoro HS, Abidemi A, Ojo MM, Oguntolu FA. Mathematical model of COVID-19 pandemic with double dose vaccination. Acta Biotheor. 2023;71(2):9. doi:10.1007/s10441-023-09460-y.
19. Musa R, Peter OJ, Oguntolu FA. A non-linear differential equation model of COVID-19 and seasonal influenza co-infection dynamics under vaccination strategy and immunity waning. Healthcare Anal. 2023;4(5):100240. doi:10.1016/j.health.2023.100240.
20. World of Health Organization. Coronavirus disease (COVID-19): similarities and differences between COVID-19 and influenza. Available from: https://www.who.int/news-room/questions-and-answers/item/coronavirus-disease-covid-19-similarities-and-differences-with-influenza. [Accessed 2024].
21. Bhowmick S, Sokolov IM, Lentz HHK. Decoding the double trouble: a mathematical modelling of co-infection dynamics of SARS-CoV-2 and influenza-like illness. Biosystems. 2023;224(11):104827. doi:10.1016/j.biosystems.2023.104827.

22. Ojo MM, Benson TO, Peter OJ, Goufo EFD. Nonlinear optimal control strategies for a mathematical model of COVID-19 and influenza co-infection. Phys A: Stat Mech Appl. 2022;607(1):128173. doi:10.1016/j.physa.2022.128173.
23. Butt AIK, Imran M, McKinney BA, Batool S, Aftab H. Mathematical and stability analysis of dengue malaria co-infection with disease control strategies. Mathematics. 2023;11(22):4600. doi:10.3390/math11224600.
24. Butt AIK, Aftab H, Imran M, Ismaeel T, Arab M, Gohar M, et al. Dynamical study of lumpy skin disease model with optimal control analysis through pharmaceutical and non-pharmaceutical controls. Eur Phys J Plus. 2023;138(11):1048. doi:10.1140/epjp/s13360-023-04690-y.
25. Ojo MM, Benson TO, Shittu AR, Goufo EFD. Optimal control and cost-effectiveness analysis for the dynamic modeling of Lassa fever. J Math Comput Sci. 2022;12:136.
26. Ayele TK, Doungmo Goufo EF, Mugisha S. Mathematical modeling of HIV/AIDS with optimal control: a case study in Ethiopia. Results Phys. 2021;26(1):104263. doi:10.1016/j.rinp.2021.104263.
27. Burden R, Faires J. Numerical analysis. 9th ed. Boston, MA, USA: Cengage Learning; 2011.
28. Butt AIK, Chamaleen DBD, Batool S, Nuwairan MA. A new design and analysis of optimal control problems arising from COVID-19 outbreak. Math Meth Appl Sci. 2023;46(16):16957–82.
29. Martchva M. An introduction to mathematical epidemiology. New York, NY, USA: Springer; 2015.
30. Butt AIK, Imran M, Aslam J, Batool S, Batool S. Computational analysis of control of hepatitis B virus disease through vaccination and treatment strategies. PLoS One. 2023;18(10):e0288024. doi:10.1371/journal.pone.0288024.
31. Castillo-Chavez C, Feng Z. Global stability of an age-structure model for TB and its applications to optimal vaccination strategies. Math Biosci. 1998 Aug 1;151(2):135–54. doi:10.1016/S0025-5564(98)10016-0.
32. Ahmad W, Rafiq M, Abbas M. Mathematical analysis to control the spread of Ebola virus epidemic through voluntary vaccination. Eur Phys J Plus. 2020;135(10):1–34. Article no. 775. doi:10.1140/epjp/s13360-020-00683-3.
33. Musa SS, Zhao S, Abdulrashid I, Qureshi S, Colubri A, He D. Evaluating the spike in the symptomatic proportion of SARS-CoV-2 in China in 2022 with variolation effects: a modeling analysis. Infect Dis Model. 2024;9(2):601–17. doi:10.1016/j.idm.2024.02.011.
34. Abdulrashid I, Friji H, Topuz K, Ghazzai H, Delen D, Massoud Y. An analytical approach to evaluate the impact of age demographics in a pandemic. Stoch Environ Res Risk Ass. 2023;37(10):3691–705. doi:10.1007/s00477-023-02477-2.
35. Abdulrashid I, Caraballo T, Han X. Effects of delays in mathematical models of cancer chemotherapy. J Pure Appl Funct Anal. 2022;7(4):1103–26.
36. Borri A, Palumbo P, Papa F, Possieri C. Optimal design of lock-down and reopening policies for early-stage epidemics through SIR-D models. Annu Rev Control. 2021;51(29):511–24. doi:10.1016/j.arcontrol.2020.12.002.
37. Borri A, Palumbo P, Papa F. The stochastic approach for SIR epidemic models: do they help to increase information from raw data? Symmetry. 2022;14:2330. doi:10.3390/sym14112330.